USING NANOTECHNOLOGY IN VISCOELASTIC SURFACTANT STIMULATION FLUIDS

A Thesis

by

MERVE RABIA GURLUK

Submitted to the Office of Graduate Studies of
Texas A&M University
in partial fulfillment of the requirements for the degree of

MASTER OF SCIENCE

Approved by:

Chair of Committee,	Hisham A. Nasr-El-Din
Committee Members,	Robert H. Lane
	Mahmoud El-Halwagi
Head of Department,	A. Daniel Hill

December 2012

Major Subject: Petroleum Engineering

ABSTRACT

Viscoelastic surfactant (VES) fluids are preferred for many applications in the oil industry. Their viscoelastic behavior is due to the overlap and entanglement of very long wormlike micelles. The growth of these wormlike micelles depends on the charge of the head group, salt concentration, temperature, and the presence of other interacting components. The problem with these fluids is that they are expensive and used at temperatures less than 200°F.

The viscoelasticity of nanoparticle-networked VES fluid systems were analyzed in an HP/HT viscometer. A series of rheology experiments have been performed by using 2-4 vol% amidoamine oxide surfactant in 13 to 14.2 ppg $CaBr_2$ brines and 10.8 to 11.6 ppg $CaCl_2$ brines at different temperatures up to 275°F and a shear rate of 10 s^{-1}. The nanoparticles evaluated were MgO and ZnO at 6 pptg concentration. In addition, the effect of different nanoparticle concentrations (0.5 to 8 pptg) and micron size particles on the viscosity of VES fluid was investigated. The oscillatory shear rate sweep (100 to 1 s^{-1}) was performed from 100 to 250°F. The effect of fish oil as an internal breaker on the viscosity of VES micelles was examined.

This study showed that the addition of nanoparticles improved the thermal stability of VES micellar structures in $CaBr_2$ and $CaCl_2$ brines up to 275°F and showed an improved viscosity yield at different shear rates. Micro- and nanoparticles have potential to improve the viscosity of VES fluids. Lab tests show that for VES micellar systems without nanoparticles, the dominant factor is the storage modulus but when

nanoparticles are added to the system at 275°F the loss modulus becomes the dominant factor. These positive effects of nanoparticles on VES fluid characteristics suggest that these particles can reduce treatment cost and will exceed temperature range to 275°F. With this work, we hope to have better understanding of nanoparticle/viscoelastic surfactant interaction.

DEDICATION

To my parents, brother and sister

ACKNOWLEDGEMENTS

I owe my deepest gratitude to my advisor, Dr. Hisham A. Nasr-El-Din, for his encouragement, guidance, effort and giving me the freedom to pursue my own ideas during my thesis. Without his guidance, my research would not have been possible.

I would also thank my committee members, Dr. Robert Lane, Dr. Mahmoud El-Halwagi, for their guidance and support throughout the course of this research.

In addition, my sincere thanks also goes to Mr. Crews, who helped me understand the topic, and answered my questions every time.

I am indebted to my company, BOTAS (Petroleum Pipeline Corporation), for funding me, and giving me an opportunity to do my Master's degree in petroleum engineering.

Thanks also go to my friends and colleagues and the department faculty and staff for making my time at Texas A&M University a great experience.

Finally, I would like to thank my mother and father for their encouragement to pursue this degree and to my sister and brother for their favor all the time.

TABLE OF CONTENTS

Page

LIST OF FIGURES

LIST OF TABLES

CHAPTER I

INTRODUCTION

The improvement of oil production is becoming more crucial because of the rapid increase in the oil demand. Geologic formations may contain large quantities of oil or gas, but have a poor flow rate due to low permeability, or from damage to the rock pore space during either drilling or production. Matrix acidizing and hydraulic fracturing are major stimulation processes used to handle these limitations. Hydraulic fracturing involves the injection of more than a million gallons of water, sand and chemicals at high pressure down and across into horizontally drilled wells to fracture a subterranean formation. The pressurized mixture causes the rock layer, to crack. When the applied pump rates and pressures are decreased or removed from the formation, the crack or fracture cannot close completely due to the high permeability proppant. The sandstone and siltstone formations are hydraulically fractured with a variety of fluids such as high concentration crosslinks, linear gels, polyacrylamide slick waters and even treated fresh water. Although these fluids are economical, they can cause severe damage during the stimulation process and do not offer the advantages of an all-inclusive system (Yu et al., 2010; Leitzell, 2007; Crews et al., 2008).

Polymer-based fluids have been used as completion and fracturing fluids in the oil industry to stimulate oil and gas wells. The problem related to polymer-based fluids is that they leave a polymer residue in the formation. This has a negative impact on the fracture permeability. According to studies, fish eyes or microgels present in some

polymer gelled carrier fluids will plug pore throats, causing impaired leak-off, and then formation damage (Crews et al., 2008).

For the last decade, viscoelastic surfactants have been used in stimulation, completion and fracturing fluids due to their rheological properties. Using VES fluid, which is tolerant to high-density brines like $CaCl_2$, $CaBr_2$, KCl and NH_4Cl leads to the increase in viscosity and formation of a pseudo-filter cake. However, excessive fluid leak-off and poor thermal stability limitations precluded widespread use in fracture treatments (Crews et al., 2006; Crews et al., 2010).

A method or a composition should be found to make the system stabilizers more effective in stabilizing the viscosity of VES fluid, particularly the gelled fluid which has leaked off into the treated reservoir, and to reduce such leak-off.

1.1 Problem Statement

Viscoelastic surfactant (VES) fluids are preferred nowadays for many applications in the oil field industry. Their viscoelastic behaviors are dependent on the overlap and entanglement of very long worm like micelles. The problem with this fluid is that they are expensive and used for fracture-pack temperatures up to about 200°F. VES fluids do not form a filter cake on the formation face because the viscosity of VES fluids is based on the arrangement of low molecular weight surfactants and not high molecular weight polymers like guar and hydroxypropyl guar. Therefore, they leak into the reservoir matrix (Crews et al., 2006). Due to poor fluid efficiency of VES fluid, the permeability of a reservoir is generally less than 400 md and more total fluid volume is

required for a given treatment. In addition, a larger amount of leaked off fluid within the reservoir matrix occurs, which needs to be removed after the treatment (Huang & Crews, 2007).

VES fluid has been considered to break by two methods: contact with reservoir hydrocarbons or contact and dilution with reservoir brine. However, relying on these methods to break down the leaked-off VES fluid to achieve quick and complete treatment fluid flow back is questionable, especially for dry gas reservoirs. Therefore, there is a need in the petroleum industry to have a better system that overcomes these problems (Huang & Crews, 2007).

1.2 Research Objectives

- To investigate the rheological properties of viscoelastic surfactant fluid systems with and without nanoparticles
- To analyze the effects of particle size and composition on viscoelastic surfactant fluid systems.
- To study the effects of temperature, type and amount of salinity on viscoelastic surfactant fluid systems.
- To study the effect of an internal breaker.

1.3 Surfactants

Surfactants (surface active agents) consist of two parts: a polar (hydrophilic) head group that likes water and nonpolar (hydrophobic) tail group that dislikes water, as shown in **Fig. 1**. In a micelle, the hydrophobic tails form the core of the aggregate and the hydrophilic heads are in contact with the solvent. When a surfactant adsorbs from aqueous solution at a hydrophobic surface, it directs its hydrophobic group towards the surface and exposes its polar group to the water. The surface has become hydrophilic; as a result, the interfacial tension between the surface and water has been reduced (Holmberg et al., 2003). The head-group can be ionic, so that the molecule becomes charged by dissociation in aqueous solution; or nonionic, in which case the amphiphile remains uncharged. Zwitterionic head-groups, with two charges of opposite sign, are also common. The hydrophobic tail is always a short hydrocarbon (though fluorocarbons can also be used); in some cases (such as biological lipids) there are two tails.

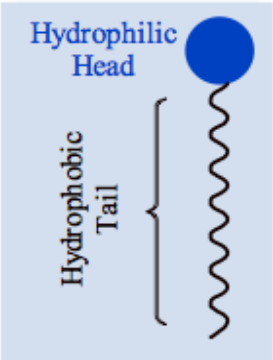

Fig. 1—Schematic representation of different types of surfactants.

The hydrophobic part of a surfactant may be branched or linear. The polar head group is usually attached at one end of the alkyl chain. The physicochemical properties of the surfactant depend on the degree of chain branching, the position of the polar group and the length of the chain. The polar part of the surfactant may be ionic or non-ionic (Zana et al., 2005). Surfactants are characterized by their tendency to adsorb at surfaces and interfaces. They are used for providing stability to dispersions of colloidal particles (Goodwin, 2009).

1.4 Adsorption of Surfactants at Solid/Liquid Interfaces

The driving force for a surfactant to adsorb at an interface is to decrease the free energy of that phase boundary, which indicates the amount of work required to expand the interface. When the boundary between water and the air is covered by surfactant molecules, the surface tension is reduced. In addition, as the surfactant packing at the interface is denser, the reduction in surface tension becomes larger.

The adsorption of surfactants on solids is affected by the variation in the molecular structures, and the conditions of the solution, such as pH, ionic strength, and temperature. As the number of hydrophobic chains increases, the adsorption density because of the stronger hydrophobic chain-chain interaction, while as the number of hydrophilic head groups increases results in the decrease in the adsorption since the larger head groups have larger surface area. For ionic surfactants, the adsorption mainly depends on the pH of the solution because it determines the solid charges. The addition of salts in the system may result in a reduction in the adsorption of ionic surfactant on

the oppositely charged solid because salts screen the electrostatic repulsion. When temperature increases, the adsorption of ionic surfactant usually decreases (Lu, 2008).

The main property of a surfactant is the tendency to accumulate at interfaces. The degree of surfactant concentration depends on the surfactant structure and the nature of two phases, meeting at the interface. To select a good surfactant, it should have low solubility in the bulk phases (Holmberg et al., 2003).

1.5 Surfactants Aggregate in Solution

Surface active agents tend to form aggregates, called micelles. Micelle formation is an alternative mechanism to adsorption at the interfaces for taking off hydrophobic groups from contact with water, so decreasing the free energy of the system. Only surfactant unimers attribute to decrease in surface and interfacial tension, and the concentration of free unimers in solution controls dynamic phenomena.

Micelles are generated at very low surfactant concentrations in water. The concentration at which micelles start to form is called the critical micelle concentration, or CMC. The unimer concentration will never exceed the critical micelle concentration, regardless of the amount of surfactant added to the solution (Holmberg et al., 2003).

The variation of the CMC with the surfactant chemical structure leads to these results:

1- The CMC decreases with increasing alkyl chain length of the surfactant. Generally, the CMC decreases by a factor of ca. 2 for ionics and by a factor of ca. 3 for non-ionics on adding one methylene group to the alkyl chain.

2- The critical micelle concentrations of non-ionics are lower than those of ionics.

3- Cationics have a bit higher critical micelle concentrations than anionics.

4- Monovalent inorganic counterions give the same CMC while increasing the valency to 2 causes the reduction of the CMC by approximately a factor of 4. Organic counterions decrease the CMC when compared with the inorganic ones.

5- Alkyl chain branching, double bonds, aromatic groups and some other polar character in the hydrophobic part generate changes in the CMC, whereas a significant decrease of the CMC results from perfluorination of the alkyl chain.

The added electrolyte has an effect on the CMC of ionics. The CMC decreases with the salt addition. The effect is larger for long-chain surfactants than short-chain ones. Consequently, the change of CMC with the number of carbons in the alkyl chain at high salt concentrations is much stronger than without added salt. The effect of salt addition depends on the valency of the ions and added counter-ions (Holmberg et al., 2003). Wormlike micelles can form at ambient temperature using cationic surfactants. At high surfactant concentrations, spherical aggregates turn into cylindrical aggregates because of electrostatic forces. The addition of cosurfactants or other low molecular weight additives can promote the growth of the aggregates. These are:

A- Surfactant and simple salt: Simple salts such as sodium chloride (NaCl) or potassium bromide (KBr) are added to ionic surfactant solutions, causing the screening of the electrostatic interactions between the charges, and thus in the growth of the aggregates.

B- Surfactant and cosurfactant: The ratio between the alcohol and surfactant concentrations controls the polymorphism of the self-assembly (Berret, 2004).

C- Surfactant and strongly binding counterion: Strongly binding counterions, hydrotopes, are small molecules that have opposite charge with respect to that of the surfactant. Hydrotopes like salicylate and chlorobenzoate counterions, contain an aromatic phenyl group. CTAB and CPCl with sodium salicylate (NaSal) micellar systems have generally been studied during the last two decades (Rehage and Hoffmann, 1991; Nash, 1958; Larsen et al., 1973; Hyde and Johnstone, 1975; Ulmius et al., 1979; Hoffmann et al., 1981). In CPCl-NaSal system, long wormlike micelles are formed at the critical micelle concentration (0.04 wt. %) (Bijma and Engberts, 1997; Bijma et al., 1998; Göbel and Hiltrop, 1991).

D- Amphoteric surfactant: Amphoteric surfactants contain both positive and negative charges in the head group. They associate at low concentrations and aqueous solutions exhibit strong gel-like properties, resulting from the generation of an entangled network of micelles (Fischer et al., 1994; Fischer et al., 2002).

E- Gemini surfactants and surfactant oligomers. The covalent binding of amphiphilic moieties at the level of the head group results in the forming of gemini surfactants and surfactant oligomers (In, 2001). In aqueous solutions, these molecules have a polymorphism of aggregation (Buhler et al., 1997; Oda et al., 1997; Oda et al., 1999; In. et al., 2001; Oelschlaeger et al., 2003). Cylindrical micelles get close to each other and form rings in gemini surfactants, leading to large end-cap energies (In et al., 1999).

F- Cationic and anionic mixtures: Surfactants, oppositely charged, have enhanced the rheological properties, and through the formation of mixed wormlike micelles. The growth of the micelles is assumed to arise from the charge neutralization of the surface potential and from the related increase of the ionic strength (Kaler et al., 1992; Koehler et al., 2000).

1.6 Packing of Surfactant Molecules in Micelles

The shapes of surfactant aggregates can be predicted based on the packing parameter, a method to correlate the molecular geometry with the growth of micelles (Tanford, 1980; Israelachvili et al., 1975).

$$P = \frac{V}{a_0 l}$$

where V is the volume of surfactant molecule, a_0 is the optimal cross-sectional area of hydrophilic group and l is the hydrocarbon length.

Different values of the packing parameter cause different critical packing shapes, and therefore different arrangement of the surfactant molecules as shown in **Fig. 2**. When the packing parameter is smaller than 1/3, spherical micelles may be formed; when it is between 1/3 and 1/2, cylindrical micelles may be generated; when it is greater than 1/2, bilayer and vesicles may be formed.

Total surfactant concentration, the type of surfactants used, and salinity contribute to the packing parameter (Rehage and Hoffmann, 1988; Lequeux and Candau, 1994).

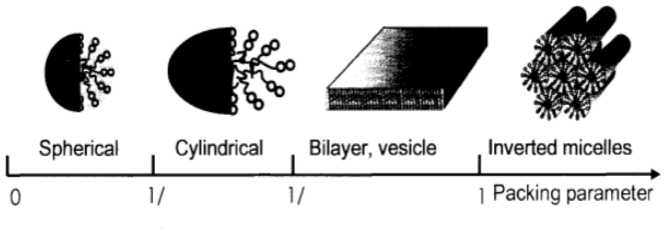

Fig. 2—Packing shapes arranged by different values of the packing parameter.

1.7 Kinetics of Micellization

1.7.1 Aniansson and Wall Theory of Micellar Kinetics

The driving force of micelle formation is the elimination of the contact between the alkyl chains and water. As a spherical micelle gets larger, it becomes more efficient because the ratio of the volume-to-area increases. Decreasing the micelle size causes an increase in hydrocarbon-water contact (Holmberg, 2003).

Dilute micellar solutions are characterized by two relaxation processes. They contribute to the fast process of the exchange of a surfactant A between micelles A_s and A_{s-1} as in reaction, with the rate constants of association, k_s^+ and dissociation, k_s^-:

$$A_{s-1} + A \xleftrightarrow{k_s^+,\ k_s^-} A_s$$

The slow process represents the micelle formation/breakdown. It is assumed that this reaction takes place via a series of stepwise reactions and does not include the contribution of the counterions. The micelles undergo a fast equilibration according to exchange reaction, where each micellar species gains or loses a small number of monomers. This process causes a shift of the range of micelles proper of the distribution.

They used a model of micellar solutions at higher surfactant concentrations than critical micelle concentration, based on the above distribution curve of the micelle aggregation number (N) as shown in **Fig. 3**. This curve is plotted as a concentration of aggregates A_s, against s. When the s is equal to N, this corresponds to the micelles proper.

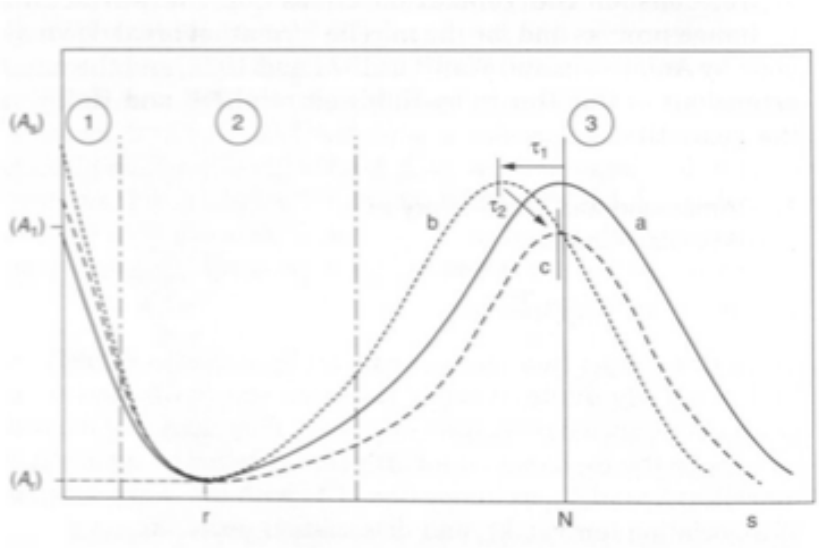

Fig. 3—Distribution curve of the micelle aggregation number and its modifications.

The micelles proper have a fast equilibration according to the reaction, where each micelle gains or loses a small number of monomers. This causes a shift of the distribution of the micelles proper from the initial curve a to curve b. The distribution curve c, corresponds to the final state of the system and contains the formation or breakdown of some micelles (Zana et al., 2005).

The rate constant, k_s^+, is diffusion controlled and depends on surfactant and micelle size. On the other hand, the rate constant, k_s^-, is dependent on alkyl chain length.

Two relaxation times are determined to characterize molecular processes in micellar solutions: τ_1 measures the rate where surfactant molecules exchange between micelles, while τ_2 measures the rate where micelles form and disintegrate (Holmberg, 2003).

Aniansson and Wall indicated that the similarity between micellar kinetics and diffusion phenomena has been supported by giving the rate equations corresponding to reaction, the relative concentration change upon perturbation, and the quantity J_s, as a flux:

$$\xi_s = \{ [A_s] - [A_s]^{eq} \} / [A_s]^{eq}$$

$$J_s = -k_s^- [A_s]^{eq} [\xi_s - \xi_{s-1}(1+\xi_1) - \xi_1]$$

where $[A_s]^{eq}$ is the equilibrium concentration of A_s.

For the assumptions of small perturbations and large s in size distribution curve, the rate equations become

$$J_s = -k_s^- [A_s]^{eq} \left(\frac{\delta \xi_s}{\delta s} - \xi_1 \right) \quad and \quad -\frac{\delta J_s}{\delta s} \cong [A_s]^{eq} \frac{\delta \xi_s}{\delta t}$$

These equations are similar with Fick's laws for diffusion in a tube.

Relaxation Time For the Exchange Process

These assumptions were made by Aniansson and Wall:

1- The amplitude of the perturbation is small.

2- The exchange of surfactants between oligomers and micelles does not occur during the exchange process.

3- Around the maximum, the shape of the distribution curve is Gaussian for dilute solutions, and σ^2 shows the variance of the distribution.

$$[A_s] = [A_s]^0 \exp\left[-(N-s)^2 / 2\sigma^2\right]$$

4- The rate constants are independent of s and equal to k+ and k- in the micelles proper, which causes that the spectrum of relaxation times related to fast process turns to a single relaxation time, shown by

$$1/\tau_1 = (k^- / \sigma^2) + (k^- / N)a$$

In this equation, N is the average micelle aggregation number and a is the reduced surfactant concentration.

$$a = (C - [A_1]^{eq}) / [A_1]^{eq}$$

The free surfactant concentration may be taken as the cmc for a first approximation (Israelachvili et al., 1976).

The main assumption made by Aniansson and Wall is that micelles form or break down with a series of stepwise reactions. The aggregation space is divided into three parts. The first part ($1 \le s \le s_1$) corresponds to the oligomers; the second part ($s_1 < s < s_2$) is for premicellar aggregates; and the last part ($s \ge s_2$) is for the micelles proper. The contribution of part 2 to the mass balance equation is negligible and the flux

J_s in part 2 is not dependent on s. The following equation was obtained with these assumptions and at concentrations above critical micelle concentration:

$$1/\tau_2 = N^2\{R[A_1]^{eq}[1+(\sigma^2/N)a\}^{-1} \quad \text{and} \quad R = (\sum_{s_1+1}^{s_2}(k_s^-[A_s]^{eq})^{-1}$$

R refers to a resistance against the transfer of monomers between part 1 and 3. To get information about the species present at very low concentrations, τ_2 can be used because R is dependent on the concentrations of the species in part 2.

Extension of the Theory to Ionic Surfactants with or without Added Salt

When the salt is added to ionic surfactants, this equation is used:

$$1/\tau_1 = (k^-/\sigma^2) + (k^-/N)aF \quad \text{and} \quad F = 1 + (1-\alpha)^2/(1+\alpha a) + 2\gamma'[A_1]^{eq}$$

In the above equation, is the accessible micelle ionization degree done by experimentally and $\gamma' = 0.587/b(1+b)^2$ with $b = ([A_1]^{eq} + m_s)^{0.5}$ where m_s is the concentration of added salt. The assumption $[A_1]^{eq} \cong cmc$ is not valid for ionic surfactants. Electrochemical measurements using surfactant ion-specific electrodes provides determining the $[A_1]^{eq}$ at each value of the concentrations of surfactant and added salt.

Lessner et al. (1981) suggested the below equation to determine τ_2 for ionic surfactant solutions in the presence of added electrolyte.

$$1/\tau_2 = N^2(1+\mu)/\{R[A_1]^{eq}[1+(1+\mu)(\sigma^2/N)+(k^-/N)a]\}$$

where $\mu = (1+\alpha)^2[A_1]^{eq}/[X]$, [X] is the concentration of free counterions.

Kahlweit et al. shows the contribution of coagulation reactions to the theory of the dynamics of the micelle formation/breakdown process where the intermicellar interactions are attractive.

$$A_s \longleftrightarrow A_i + A_j$$

$$A_{s-1} + A \xleftrightarrow{k_s^+,\ k_s^-} A_s$$

$$1/\tau_2 = 1/\tau_{21} + 1/\tau_{22}$$

τ_{22} corresponds to the first reaction and τ_{21} corresponds to the second reaction. They are given by

$$1/\tau_{22} = \beta N a / [1 + (\sigma^2 / N)a]$$

where β is a measure of the mean dissociation rate constant.

$$1/\tau_2 = Q_1([X]/[A_1]^{eq})^{-q_1} + Q_2([X]/[X]_0)^{q_2}$$

Q_1, Q_2 are two constants; $[X_0]$ is the concentration of free counterions at the beginning of coagulation; and q_1, q_2 are two positive numbers.

Kahlweit et al. (1985) thought that the probability of micelle breakdown was not dependent on the surfactant concentration. In addition, it was assumed that reactions consist of the premicellar aggregates in part 2.

Turner and Cates (1990) generated an exponential distribution of micelle lengths and a rate constant of micelle fragmentation (k_b, (s.unit length)$^{-1}$) that is proportional to the mean micelle length <L>. The relaxation time is given by

$$1/\tau_2 = 2k_b < L >$$

Waton obtained the general equation for this relaxation time and this equation can be used for different types of distribution of micelle lengths.

$$1/\tau_2 = k_f / [d \log N / d \log(C - cmc)]$$

where k_f is the mean rate constant of fragmentation.

1.8 Nanotechnology

The revolution of nanotechnology has aroused a great interest for its many applications in the oil & gas industry such as enhanced oil recovery. Nanotechnology represents the development and application of materials, methods, and devices, in which critical length scale is on the order of 1–100 nm. Nanotechnology is concerned with materials and systems whose structures and components exhibit novel and significantly improved physical, chemical, and biological properties, phenomena, and processes due to their nanoscale size (Huang and Crews, 2008).

Nanotechnology has two distinct advantages:

1. It offers the possibility of creating materials with dimensions on the nanoscale.

2. Devices in the nanoscale need less material to make them and use less energy. Their function may be enhanced by reducing the characteristic dimensions (Ramsden, 2011).

The nanoparticles are inorganic crystals that do not dissolve in water, oil, or solvent (Huang and Crews, 2008). Some unique nanoparticles have been applied to

viscoelastic surfactant fluid systems to improve their performance as fracturing and fracture-packing fluids (Yu et al., 2010; Pourafshary et al., 2009).

CHAPTER II

LITERATURE REVIEW

2.1 Viscoelastic Surfactant Fluids

Surfactants are used to reduce surface tension, change wettability, mobilize residual oil, and disperse corrosion inhibitors. They have a wide scope of applications due to the ability of surfactants to adsorb on various surfaces and form micellar structures (Nasr-El-Din et al., 2003).

The surfactant based viscoelastic (VES) fluid systems are under the category of polymer-free fluids and have been widely used for hydraulic fracturing operations over the past years (Samuel et al. 1997; Mathis et al. 2002; Leitzell 2007). These fluids leave no residue and facilitate rapid flowback (Gupta 2009). For VES fluids, elasticity plays an important role in suspending the proppants.

Viscoelasticity is the property of materials that exhibit both viscous and elastic characteristics when undergoing deformation. An elastic response can occur when a mechanical force causes reversible sample deformation. During the deformation process, elastic energy is stored in the sample. In contrast to this, viscous properties are observed when an external force can be dissipated as heat because of flow processes. The viscoelastic properties are resulted from shearing forces (Zana et al., 2005). The viscoelastic fluid acts as a viscous pseudo-plastic fluid under steady state conditions, whereas the fluid shows an elastic behavior under a higher shear (Gogarty, 1974; Hoey et al., 2003).

The aggregates in viscoelastic surfactant solutions have been characterized by static and dynamic light scattering, electric birefringence, flow birefringence, nuclear magnetic resonance, rheological, kinetic, and neutron-scattering experiments (Zana et al., 2005).

2.2 Colloid Stability and the Role of Surface Forces

A tiny particle of one phase dissolved in another is referred to as a colloidal solution. The colloidal solutions have high surface area of the dispersed phase, and the chemistry of these interfaces is important (Pashley and Karaman, 2004).

The colloid stability of dispersions, emulsions and foams is governed by the balance of three main forces: (1) van der Waals attraction results from the London dispersion forces between the particles or droplets; (2) double layer repulsion that forms when using ionic surfactants or polyelectrolytes; and (3) steric repulsion that arises when using adsorbed nonionic surfactants or polymers (Tadros, 2009).

2.2.1 Van der Waals Attraction

Atoms or molecules always attract each other at short distances of separation because of Van der Waals forces. The three different types of attractive forces are: dipole–dipole interaction (Keesom), dipole-induced dipole interaction (Debye) and London dispersion force. The London dispersion force occurs for polar and nonpolar molecules and results from fluctuations in the electron density distribution (Tadros, 2007; Tadros, 2009).

The attractive energy between two atoms or molecules is inversely proportional to the sixth power of interatomic distance r:

$$G_a = -\frac{\beta_{11}}{r^6}$$

where β_{11} the London dispersion constant.

For colloidal particles, consisting of atom or molecular assemblies, the attraction energies may be added:

$$G_A = -\frac{AR}{12h}$$

where A is the effective Hamaker constant.

$$A = (A_{11}^{1/2} - A_{22}^{1/2})^2$$

where A_{11} is the Hamaker constant between particles in vacuum and A_{22} the Hamaker constant for equivalent volumes of the medium:

$$A = \pi q^2 \beta_{ii}$$

where q is number of atoms or molecules per unit volume. From Fig. 4, G_A decreases with the increase in the separation distance (h).

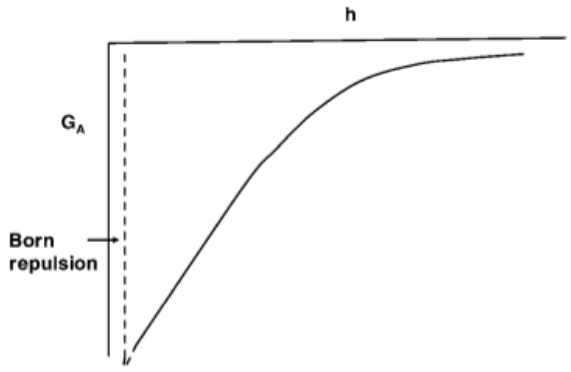

Fig. 4—Variation of the Van Der Waals attraction energy with separation distance.

2.2.2 Electrical Double Layer Repulsion

Electrical double layers are produced when ionic surfactants are used. Repulsive forces between the dissociated ions and a much stronger attraction back to the surface will occur because of the high electric field generated by a high density of ions dissociated from the surface. The electrical field generated at the surface eliminates leaving the dissociated ions from the surface region, and these ions as well as the charged surface form a diffuse electrical double layer, as shown in Fig. 5 (Pashley and Karaman, 2004; Tadros, 2007).

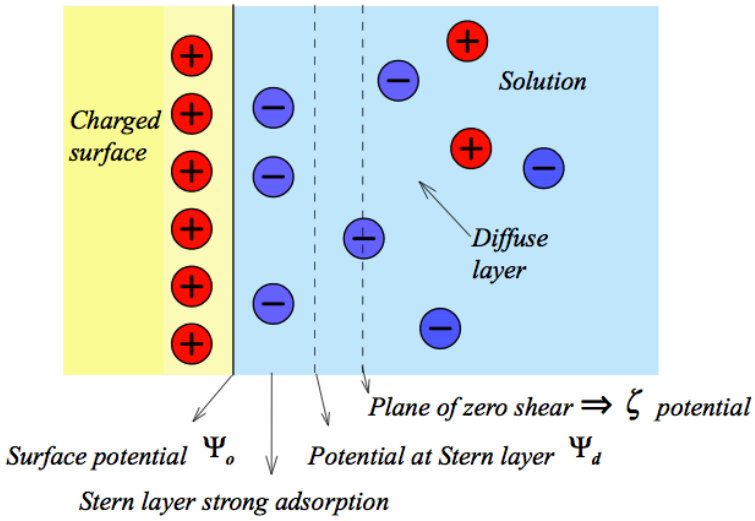

Fig. 5—The electrical field produces at the surface.

Gouy and Chapman proposed the diffuse double layer. A surface charge is produced from the head group of the ionic surfactant on adsorption of the molecules on particles. This surface charge σ_0 results from unequal distribution of counterions and co-ions. Stern introduced the adsorbed counter ions in the fixed first layer. The potential at the surface ψ_0 decreases at a point and then exponentially with a decrease in distance x.

The electrolyte concentration and valency of the counterions affect the double layer extension:

$$\frac{1}{\kappa} = \left(\frac{\varepsilon_r \varepsilon_0 kT}{2n_0 Z_i^2 e^2}\right)^{\frac{1}{2}}$$

where ε_r is the dielectric constant, ε_0 is the dielectric constant of free space, k is the Boltzmann constant, T is the absolute temperature, n_0 is the number of ions per unit

volume of each type present in bulk solution, Z_i is the valency of the ions, e is the electronic charge (Tadros, 2007; Tadros, 2009).

The Hofmeister series ranks the relative influence of ions on the physical behavior of colloidal systems. The series for monovalent cations and anions is as follows:

$$Cs^+ > Rb^+ > K^+ > Na^+ > Li^+$$

$$CNS^- > I^- > Br^- > Cl^- > F^- > NO_3^- > ClO_4^-$$

When the size of the ion is small, this results in a higher charge density for cations. The larger anions increase the adsorption (Zang and Cremer, 2006; Goodwin, 2009). When charged colloidal particles in a dispersion approach each other, the double layers start to overlap and repulsion occurs. The potential decay is not completed because of the limited space; therefore, the individual double layers cannot develop as illustrated in Fig. 6.

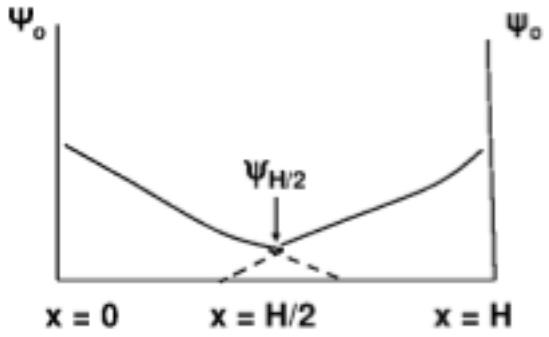

Fig. 6—The double layer interaction for two flat plates.

For two spherical particles of radius R and surface potential Ψ_0 and condition $\kappa R<3$, the expression for the electrical double layer repulsive interaction (G_{el}) is given by the following expression:

$$G_{el} = \frac{4\pi\varepsilon_r\varepsilon_0 R^2\psi_d^2 \exp(-\kappa h)}{2R+h}$$

where h is the closest distance of separation between the surfaces, κ is the Boltzman constant.

2.3 Total Energy of Interaction: Deryaguin-Landau-Verwey-Overbeek (DLVO) Theory

Combination of G_{el} and G_A results in the theory of stability of colloids (DLVO theory):

$$G_T = G_A + G_{el}$$

A plot of G_T versus h represents the case at low electrolyte concentrations.

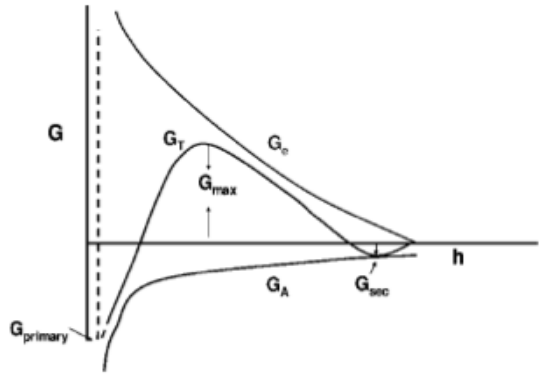

Fig. 7—The variation of G_T as a function of h according to the DLVO theory.

G_{el} decreases exponentially with h, and G_A is proportional to 1/h, as shown in **Fig. 7**. At long distances of separation, $G_A > G_{el}$, causes a minimum while at intermediate distances, $G_{el} > G_A$, results in an energy maximum, G_{max}. At low electrolyte concentrations, G_{max} is high (>25kT) and this prevents particle aggregation into the primary minimum. As the electrolyte concentration is high, the energy maximum becomes low, as represented in Fig. 8. An energy barrier resulting from the repulsive force inhibits two particles approaching one another and adhering together. When the particles have a sufficiently high repulsion (G_{max}>>kT), the dispersion will eliminate flocculation and the colloidal system will be stable.

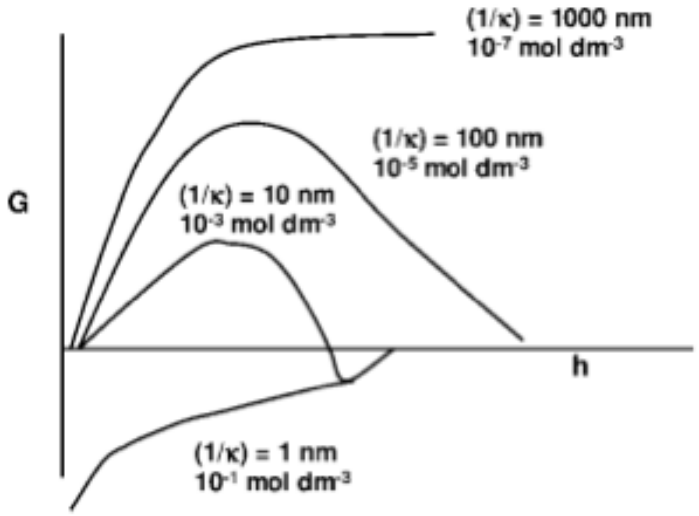

Fig. 8—The variation of G_T at various electrolyte concentrations.

Coagulation occurs at a critical electrolyte concentration, the critical coagulation concentration (ccc), which depends on the electrolyte valency. A rate constant for flocculation can be defined by; k_0= rapid rate of flocculation in the absence of an energy barrier and k= slow rate of flocculation in the presence of an energy barrier. The ratio of k_0 to k gives the stability ration, and it increases with the increase in G_{max} (Tadros, 2009).

2.4 Criteria for Stabilization of Dispersions with Double Layer Interaction

The two important criteria for stabilization are: high surface or Stern potential (zeta potential), high surface charge and low electrolyte concentration and low valency of counter- and co-ions.

The stability of many colloidal systems depends on the magnitude of electrostatic potential (ψ_0) at the surface of the colloidal particles. The zeta potential indicates the degree of repulsion between adjacent, similarly charged particles in a dispersion. The zeta potential can be calculated from the particle mobility:

$$u = \frac{v}{E/l}$$

where v is the particle velocity, E is the applied potential and l is the distance between the two electrodes; E/l is the field strength (Pashley and Karaman, 2004; Tadros, 2009).

2.5 Nanoparticle Networked VES Fluid System

The basic characteristic of surfactants is that a single molecule includes an oil-soluble hydrocarbon chain and a water-soluble group. The viscoelastic behavior of surfactants is dependent upon the overlap and entanglement of very long wormlike micelles. Wormlike micelles are elongated aggregates because of the self-assembly of surfactant molecules above the critical concentration. The growth of these wormlike micelles depends on the effective head group charge in ionic surfactants, a function of salt concentration, temperature and presence of other interacting components (Rojas et al., 2008; Huang and Crews, 2008b). The length of the wormlike micelles can be controlled by the end-cap energy and temperature. As the end-cap energy increases, the length of the micelles increases exponentially because of the high energy imposed on the system. When the end-cap energy is reduced, entropy wants to have many shorter micelles, so the length of wormlike micelles depends on the balance between the entropy and the enthalpy of the system (Van Zanten, 2011).

Salts with a hydrophobic part trigger rapid micellar growth because of their strong binding to the micelles (Nettesheim et al., 2008). The VES is compatible with a wide range of completion brines and crude oils, causing no damage to the formation (McElfresh et al., 2002). The brines can be prepared by using salts including: NaCl, KCl, $MgCl_2$, NH_4Cl, $NaBr_2$, and the other stimulation as well as completion brine salts that have a density range from 9.0 to 14.4 ppg. They can be used to increase hydrostatic pressure and lower surface treating pressure when treating deep, high-pressure reservoirs

due to the improved salinity tolerance at elevated temperatures (Crews et al., 2006; Huang et al., 2009).

A molecule acts as a dispersant by meeting these requirements. The dispersant must adsorb to the surface under the given process conditions; phase separation does not have to occur; and adequate repulsion between particles has to be maintained to inhibit agglomeration. Resistance to elastic deformation of adsorbed surfactant aggregates is the main stabilization mechanism at high ionic strength (Adler et al., 2000). The overall stability for any system is a balance of particle/interface, surfactant/interface, and particle/surfactant interactions (Hunter et al., 2008).

Adding surfactant molecules adsorbing at the oil–water interface displaces nanoparticles from the interface. Surfactant adsorption at the oil–water interface is energetically favorable and takes place on nanoparticle-stabilized emulsions with surfactant solutions. The interfacial tension decreases depending on the surfactant concentration. Above the critical micelle concentration, the complete interfacial displacement can be achieved and hence recovery of the nanoparticles from the emulsions. The application of shear stress led to the displacement of the silica nanoparticles from the interface (Vashisth et al., 2010).

Recent studies have shown the advantageous use of nanoparticles in VES fluid systems. The nanoparticles have a high surface area and display unique surface morphology and surface reactivity. They are inorganic crystals that do not dissolve in water, oil, or solvent. They strengthen the micelle-micelle interactions. A small amount of these particles is capable of maintaining viscosity at higher temperatures (up to 300°F)

and decreasing the rate of VES fluid leak-off (Huang, Crews and Willingham, 2008). Nanoparticles are smaller than the pores and pore-throat passages within a hydrocarbon reservoir so that VES fluids with nanoparticles are easily removed and cause less damage to the reservoir permeability compared with polymers (Huang and Crews, 2008c).

The addition of nanoparticles to VES fluid may improve thermal stability, keep solid suspension, and prevent phase separation by improving its solubility at high temperatures. These additives to VES systems could reduce the amount of VES surfactant required to get the stable viscosity of the fluid. (Huang and Crews, 2008b).

VES can be stabilized with a small amount of an alkali earth metal oxide and hydroxide, alkali metal oxides and hydroxides, transition metal oxides and hydroxides, post-transition metal oxides and hydroxides that reduce the amount of VES required to maintain the viscosity. These fluids exhibit no precipitation, particularly at high temperatures (Crews et al., 2008). Pyroelectric and piezoelectric crystals are good viscosity enhancers because they are small and may stay within the VES fluid that flows into the target formation. The surface charges in the pyroelectric crystals, such as ZnO nanoparticles, are generated by heating or pressing. These surface charges allow nanoparticles to associate the VES micelles to increase the viscosity by attracting the anionic part in the VES micelles (Crews and Huang, 2011; Huang et al., 2011). MgO particles and powders have been used as VES fluid stabilizers at temperatures from about 180°F to 300°F. MgO and ZnO nanoparticles have unique particle charges to crosslink with VES micelles. They may be added to VES fluids before pumping down

hole (Huang and Crews, 2008b). The MgO powder has a very high reactivity and easily reacts with water to form $Mg(OH)_2$. Therefore, water is not an appropriate carrier for them. Manipulating these particles is very difficult in pumping. In addition, the dust formed may be a problem. Propylene glycol, miscible in the water, was found as a suitable carrier fluid. It generates a microemulsion that improves suspension of high concentrated particles (Huang and Crews, 2008c).

Dual-function nanoparticles may be used for reducing fines migration and identification of a particular zone in a well. These nanoparticles can be tagged with a detectable material that is different from the composition of the primary nanoparticle component. Tagged material of the nanoparticles may provide identification of a particular zone (Crews et al., 2010).

Nettesheim et al. (2008) investigated the effect of nanoparticle addition on the properties of wormlike micellar solutions. With a combination of microrheology, small-angle neutron scattering, dynamic light scattering, and cryo-transmission electron microscopy, wormlike micellar solution of cetyltrimethylammonium bromide and sodium nitrate with 30 nm diameter silica nanoparticles was studied. At low nanoparticle concentration, the addition of the nanoparticles increases the wormlike micelle solution's zero shear rate viscosity, longest relaxation time, and storage modulus.

Rojas et al. (2008) indicated that CTAT (cationic cetyl trimethylammonium p-toluene sulfonate) mixed with SDS (anionic sodium dodecyl sulfate) had a strong synergistic effect in shear viscosity, leading to an increase in zero-shear rate viscosity for solutions with 20 mM CTAT. The crossover relaxation times of wormlike micelles of

CTAT solutions increased by the addition of SDS, and the solution became more elastic. The loading of nanoparticles improves the thermal stability of VES micellar structures in $CaCl_2$ brines to about 260°F and in $CaBr_2$ and $CaCl_2/CaBr_2$ brines to about 310°F. The formation of more thermally stable micelles will lead to use 20 to 100% less amount of VES at higher temperatures (Crews et al., 2006). Luo et al. (2012) studied an anionic fatty acid methyl ester sulfonate sodium (MES) surfactant micelle solution with pyroelectric barium titanate ($BaTiO_3$) nanoparticle, and found that this system can maintain high viscosity at elevated temperatures due to the addition of nanoparticles. The viscosity of MES micelle solution increases when the temperature increases within a certain range because of the pyroelectric effect of nanoparticles.

Huang et al. (2010) evaluated the viscous and elastic properties of conventional and nanoparticle pseudo-crosslinked wormlike micelles in brine. The base surfactant micellar fluid consisted of 13.0 ppg $CaCl_2/CaBr_2$ brine solution with 2% by volume amidoamine oxide surfactant. The pseudo-crosslinked fluid contained 35 nm diameter zinc oxide nanoparticles at 10 pptg (pound per 1000 gallon) concentration, which is about 0.08% by weight. The rheological data showed that the addition of nanoparticles increased the surfactant micellar fluid's zero shear rate viscosity more than 100 times.

Crews et al. (2010) showed that the addition of approximately 35 nm pyroelectric crystals to VES micelles could achieve viscosity at moderate, low, and ultra-low fluid shear rates. 1 vol% gel-forming surfactant with 0.046 wt% pyroelectric nanoparticles has more viscosity yield when compared with 2 vol% surfactant without nanoparticles at moderate shear rate (100 s^{-1}).

Hunter et al. (2009) studied the effects of adding silica nanoparticles to a non-ionic surfactant (TX100) on the stability and elasticity of hydrophobic silica suspensions. Results depicted that at low-to-moderate concentrations of surfactant, the stability improves with the addition of the nanoparticles at low-to-moderate surfactant concentrations.

Helgeson et al. (2010) studied the rheology of cationic wormlike micelles with like-charged nanoparticles. The formation of micelle-nanoparticle junctions acts as physical cross-links between micelles and these junctions help to have significant viscosity and elasticity in dilute and semidilute wormlike micelles. As the concentration of particles increases, the viscosity, shear modulus, and relaxation time increase and the entanglement concentration decreases. The effect of the addition of the nanoparticles on micelles can be monitored by the surface chemistry of the nanoparticles. The rheology of wormlike micelles depends on two parameters; the micellar end-cap energy, which controls the process of micellar growth and entanglement, and the micellar adsorption energy, which leads the formation of micelle-nanoparticle junctions.

Nettesheim et al. (2008) made a model to explain the association or pseudo-crosslinking of nanoparticles with elongated micelles in **Fig. 9**. The nanoparticles are initially associated with the energetically unfavorable endcaps of micelles and become the junctions of wormlike micelles. The attachment may result from the enhanced stability of the endcap curvature, the size and concentration of nanoparticles, and surface forces (Crews and Gomaa, 2012).

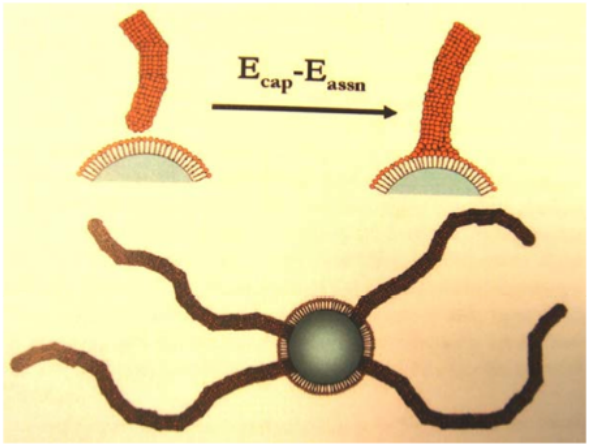

Fig. 9—The micelle particle association based on the replacement of an endcap by a nanoparticle and the resulting network junction.

Huang et al. (2008) showed that the 2 vol% non-ionic surfactant in 1.56 g/ml $CaCl_2/CaBr_2$ fluids without nanoparticles exhibited viscous-dominated behavior, while that with 0.08 wt% nanoparticles, the dominant factor was elastic modulus, resulting from strengthening of micelle-micelle associations and elongated micelle structures in the fluids.

The amount of VES in the fracturing fluid depends on generating enough viscosity to control the rate of fluid leakoff into the pores of the fractures, and producing a high viscosity to improve the size and the geometry of fractures within the reservoir (Crews and Huang, 2008). The higher fluid viscosity helps to crack the formation during fracturing operations, decrease the fluid leak-off, and carry high loading proppants to sustain the high fracture conductivity (Huang, 2008).

2.6 Internal Breaker

Internal breakers have been developed to break the surfactant gels with high surfactant concentrations. The micelles need to be converted from their rod-shaped structure into spherical ones to break them. External breakers, contacting with reservoir hydrocarbons, and dilution with reservoir brine, have been used to break VES fluids but complete treatment-fluid flowback has been a problem, especially for dry gas reservoirs (Samuel et al., 1999; Crews et al., 2006; Huang and Crews, 2008a). Water injectors can be used to decrease the concentration of the surfactants. In oil or gas wells, the surfactant gel can be mixed with a hydrocarbon phase, but mutual solvents can be used in all wells to break it (Nelson et al., 2005; Crews and Huang, 2007).

The surfactant micellar fluids have high viscosity at low shear rates and will need the high formation pressure to displace from the reservoir matrix without internal breakers (Huang and Crews, 2008a). Crews et al. (2010) indicated that internal breaker could reduce the viscosity without contacting with reservoir hydrocarbons. Figure 10 illustrates how internal breaker compounds turn thread-like micelles to non-viscous spherical shaped micelles and nanoparticles.

Crews and Huang (2007) suggested two breaking mechanisms; adding breakers to the VES fluid by degrading the compound, and using breakers that are compatible with VES fluid to degrade into VES micelles by generating compounds within the rod-like micelle structure at reservoir temperature. The second mechanism can be used over a wide temperature (80 to 300°F) and salinity range (brines up to 9.8 ppg KCL, 11.8 ppg $CaCl_2$, 14.5 ppg $CaBr_2$, and the like). The ideal breaker should break the backbone of the

surfactant to a uniform, low viscosity material that will remain soluble (Weaver et al., 2002). The use of internal breakers should improve the rate of VES fluid cleanup, and inhibit viscous emulsions from being formed when contacting with reservoir hydrocarbons.

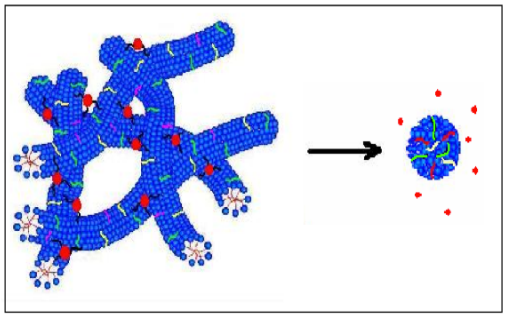

Fig. 10—The internally breaking nanoparticle pseudo-crosslinked thread-like micelles by simple micelle rearrangement.

The internal breakers with auto-oxidation properties will go inside of the micelles and the nanoparticles will associate with the micelles. When the fluid system pumps into a formation to create a fracture, the nanoparticle pseudo-crosslinked VES micelle fluid forms a wall-building pseudo-filter cake on the face of porous media to control fluid loss. When the VES micelle structures are degraded by internal breakers, the leaked-off VES fluid and the pseudo-filter cake break into brine water and nanoparticles. Internal breakers generate VES-breaking compounds over time, which penetrate and collapse the viscous, rod-like VES micelles into nonviscous, more-spherical micelles (Crews, 2005; Crews and Huang, 2007; Huang and Crews, 2008a). Since the nanoparticles are very small and easily pass through the pores of greater than 0.1 md formations, they are

flowed back with the produced fluids, and no internal or external "solids" damage is generated (Crews et al., 2010).

Organic compounds that auto-oxidize have been used for internal breakers. The organic compounds have high compatibility with thread-like micelle structures in brine. The mechanism of internal breakers depends on the auto-oxidation of select chemical bonds. During the auto-oxidation process, the organic compound breaks into hydrocarbons that can change the structure of thread-like micelles into non-viscous spherical shaped micelles. The hydrophobic organic material interacts with the surfactant hydrocarbon tails leading to dispersion at the molecular level within each thread-like micelle. The increase in the fluid temperature causes the increase in the rate of auto-oxidation of the organic material, and the rate decreases with increase in fluid salinity (Crews et al., 2010).

Crews et al. (2010) found that the fluid system with nanocrystals decreased the fluid leakoff rate by generating a viscous fluid layer of pseudo-filter cake on the face of the ceramic discs, having 400 md permeability. The small amount of viscous mineral oils develops the efficiency of the wall-building leakoff property of the nanoparticle associated thread-like micelles.

CHAPTER III

THEORY

3.1 Rheology

Rheology is the study of deformation of matter because of an applied force. The type of deformation depends on the state of matter. Gases and liquids will flow with the force, whereas the solids will deform and after removing the force, they regain their shape. The stress is the force per unit area over which it is applied and has dimensions of Pascal (Pa). The strain is the deformation relative to the original dimension and is dimensionless (Goodwin, 2009; Goodwin and Hughes, 2008).

If a fluid is considered between parallel plates as shown in Figure 11, the fluid will flow with the motion of the upper plate and exert a force across the nearest plane layer of fluid. Depending on the force per unit area (F/A), the upper layer moves with the plate, while the lower layer has no motion and intermediate layers have intermediate velocities (Schramm, 2005).

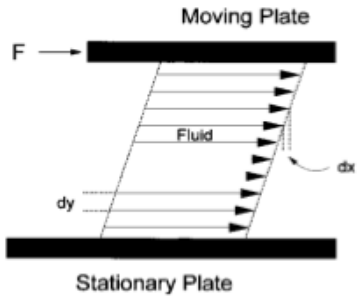

Fig. 11—The flow between parallel plates when the upper plate, of surface area A, is moved in response to a force F.

The shear stress is the force that the flowing liquid applies on a surface in the parallel direction of the flow (Larson, 1999). The displacement of a plane layer (dx) over the separation between layers (dy) is defined as the shear (dx/dy) acting on the fluid. The derivative $\frac{dV}{dy}$ shows the shear rate (Schramm, 2005).

$$dV = d(\frac{dx}{dt}) \qquad \frac{dV}{dy} = \frac{d(\frac{dx}{dy})}{dt} \tag{1}$$

Surfactants dissolved in aqueous solutions show both rheological contributions: a viscous resistance, resulting from liquid flow and an elastic response that is caused by the deformation or change of micellar structures. If the viscosity is Newtonian, the elasticity obeys Hooke's Law because the stress is directly proportional to the strain, as shown in **Fig. 12**;

$$\sigma = \eta \dot{\gamma} \tag{2}$$

where η is the viscosity (Pa.s), and is independent of the applied shear rate. At high stresses and strains, nonlinearity is seen (Goodwin and Hughes, 2008). The relationship between the relative viscosity η_r and φ was determined by Einstein for φ ≤ 0.01. Einstein assumed that the particles behave as hard-spheres with no net interaction. The viscosity increase due to the presence of the spherical aggregates can be represented by Einstein's equation:

$$\eta_r = \eta_{cmc}(1 + 2.5\varphi_m) \tag{3}$$

where

η_{cmc} indicates the viscosity of the surfactant solution at the cmc

φ_m is the volume fraction of the globular aggregates.

This equation does not include interactions, and can be used to calculate the volume occupied by the globular micelles from viscosity measurements. This law is limited to the regime of low concentrations. At higher φ-values, (0.2 > φ > 0.1) the hydrodynamic interaction should be taken into consideration for hard-spheres (Zana, 2005; Tadros, 2010).

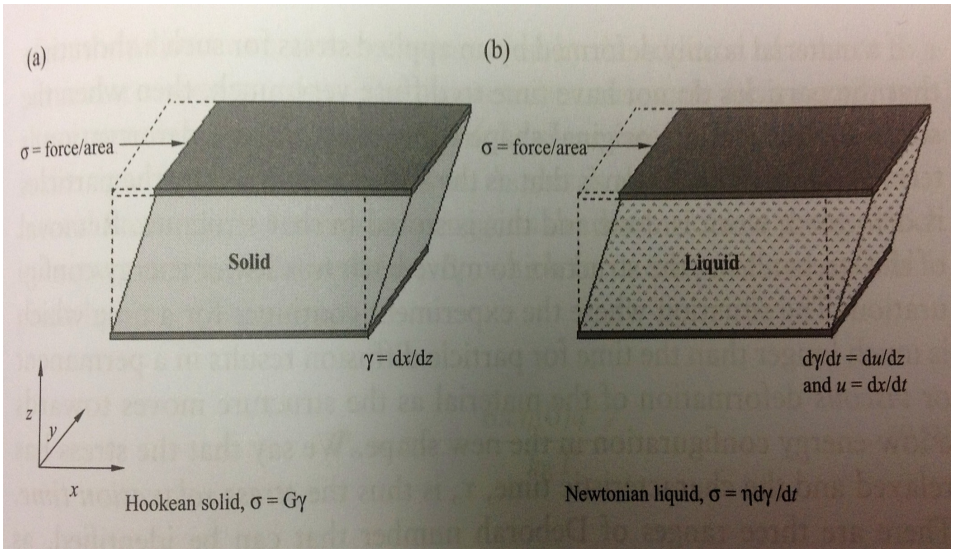

Fig. 12—The shear stress, the shear strain, and the rate of shear for (a) a Hookean solid and (b) a Newtonian liquid.

Maxwell introduced the concept of viscous flow, demonstration of the decay of elastically stored energy. This can be illustrated that all particles or droplets can diffuse to a low-energy state in a dispersion. However, if the system is deformed, the particles or droplets will be in a higher-energy state. As the system is kept in the new shape, the particles or droplets will diffuse until the original low-energy state is acquired,

that is, viscous flow has occurred.

The behavior of a viscous liquid depends on the length of time over which the relevant experiments are conducted. To stay in the linear viscoelastic region, the relaxation time must be on a time scale comparable to the experimental time. The ratio of the structural relaxation time to the experimental measurement time is given by the dimensionless Deborah number, De.

$$De = \frac{\tau}{t} \tag{4}$$

where τ is the stress relaxation time, and t is the experimental time.

According to the most rheological time-scale experiments (10^{-3}-10^{+3} s), a difference can be made between an elastic response with high relaxation times, a viscous response with very low relaxation times, and a viscoelastic response (Goodwin and Hughes, 2008; Tadros, 2010; Goodwin, 2009).

De >> 1 Elastic

De ≈ 1 Viscoelastic

De << 1 Viscous

A dimensionless number known as Péclet number, Pe, relates the shear rate of a flow to the particle's diffusion rate. The ratio of the stress applied (σ) to the thermal stress gives this number:

$$Pe = \frac{6\pi a^3 \sigma}{kT} \tag{5}$$

where k is the Boltzmann constant, T is the absolute temperature, and a is the particle radius. The shear stress should be less than 0.2 Pa to assure that the microstructure is almost undisturbed for a 100 nm colloidal particle (Wagner and Brady, 2009; Tadros, 2010).

3.1.1 Linear Viscoelastic Behavior

The linear viscoelastic behavior of entangled micellar systems show a regime of Maxwellian relaxation based on the reputation-reaction model (Cates and Fielding, 2006). Maxwellian Behavior describes the micellar dynamics. Rehage and Hoffman (1988) have used to rheology to prove that micellar growth causes an increase of the fluid viscosity. Rehage et al. discovered that a single exponential response function characterize the viscoelasticity of these surfactant solutions. The stress relaxation function represented as:

$$G(t) = G_0 \exp(-t / \tau_R) \tag{6}$$

where G_0 : elastic modulus extrapolated as $t \to 0$

τ_R : the relaxation time.

This equation shows the behavior of Maxwell fluid where the static viscosity η_0 is the product of $G_0\tau_R$. Rheological experiments are conducted as function of the angular frequency, and dynamical elastic modulus, $G^*(\omega)$ is the response function. The Fourier transform of $G(t)$ describes as:

$$G^*(\omega) = G'(\omega) + iG''(\omega) \tag{7}$$

where $G'(\omega)$ shows the storage modulus

$G''(\omega)$ shows the loss modulus.

$$G'(\omega) = G_0 \frac{\omega^2 \tau_R^2}{1+\omega^2 \tau_R^2} \qquad \text{and} \qquad G''(\omega) = G_0 \frac{\omega \tau_R}{1+\omega^2 \tau_R^2} \tag{8-9}$$

As a result of experiments, these equations have been found in viscoelastic micellar systems. It is accepted that a Maxwellian behavior indicates the wormlike character of self-assembled structures (Berret, 2004).

The Cates model suggests two primary relaxation times related to the reputation of a micelle, λ_{rep}, and micellar breakage, λ_{br}, for the dynamics of wormlike micelles. If the reptation of a micelle is larger than micellar breakage ($\lambda_{br} << \lambda_{rep}$), this causes Maxwellian linear viscoelastic rheology with a single relaxation time as the geometric mean of λ_{rep} and λ_{br}:

$$\lambda_r = \sqrt{\lambda_{rep} \lambda_{br}} \tag{10}$$

In wormlike micellar systems, typical breaking times are of the order of milliseconds.

Another method to predict the reptation-reaction kinetics model is to study the scaling properties as a function of concentration. According to the scaling laws, the reptation and breaking times both depend on the average micellar length. The loss modulus at the minimum is related to contour length and entanglement length as

$$\frac{G'_p}{G''_{\min}} \approx \frac{\bar{L}}{l_e} \qquad \text{and} \qquad G'_p = \nu k_B T \propto \frac{k_B T}{\xi_M^3} \tag{11-12}$$

where $\bar{L}$: contour length

l_e : entanglement length

ξ_M : Mesh size

ν : Network density

G'_p : The Plateau modulus

The entanglement length is dependent on the mesh size and persistence length by (Nettesheim et al., 2008)

$$l_e \approx \frac{\xi_M^{5/3}}{l_p^{2/3}} \tag{13}$$

where l_e : Entanglement length

ξ_M : mesh size

l_p : persistence length

$G''_{\min}$: Loss modulus at local minimum.

3.1.2 Non-Linear Viscoelastic Behavior

In polymer or surfactant solutions, a transition from a linear to a non-linear viscoelastic regime takes place above a critical shear rate, $\dot{\gamma}_c$. The stress is not proportional to the applied strain in non-linear regime. The flow behavior is Newtonian at rates below $\dot{\gamma}_c$, while it becomes non-Newtonian at $\dot{\gamma} \geq \dot{\gamma}_c$. This behavior has been observed for most of the wormlike micelle systems, such as CTAB and CPyCl (Berret et

al., 1998). This is because of non-homogeneous flow resulted from a mechanical instability of the shear-banding type. Two types of shear-banded flows have been suggested, the shear banding with 'top jumping', and a metastable state (Spenley et al., 1993; Berret et al., 1998; Grand et al., 1997).

Cates and co-workers developed a constitutive equation for micellar solutions based on the reptation model for steady flows with a stress tensor τ given by:

$$\tau = \frac{15}{4} G_0 (W - \frac{1}{3} I) \tag{14}$$

where W is the second moment of the distribution function (Cates, 1990; Spenley et al., 1993; Spenley et al., 1996).

Although this equation can predict the maximum behavior of the stress, the stress upturns from the solvent and disentangles chain segments at very high shear rates. However, the nonlinear differential constitutive equation was proposed by Giesekus for entangled polymer systems:

$$\begin{aligned} &(I + \alpha \frac{\lambda}{\eta_p} \tau_p).\tau_p + \lambda \tau_p(I) = \eta_p \dot{\gamma} \\ &\tau_s = \eta_s \dot{\gamma} \end{aligned} \tag{15-16}$$

where τ_p is the upper convected derivative of the stress tensor, and $\dot{\gamma}$ the rate of strain tensor and τ is the total stress given by;

$$\tau = \tau_p + \tau_s \tag{17}$$

Marrucci (1996) has developed a model that a convective constraint release mechanism has a significant effect on the non-linear flow behavior of entangled polymer systems at

high shear rates. In this model, the flow causes the disentanglement of chains at high shear rates because the thermal rate of reptation mechanism is slower than the rate of disentanglement of chains. If a convective contribution is added to the mechanism:

$$\frac{1}{\tau} = \frac{1}{\tau_0} + \dot{\gamma} \tag{18}$$

where τ is the relaxation time under flow conditions.

From this model, the rheological behavior of entangled polymers can be found, but this has never been observed for surfactant micelles.

$$\frac{\sigma_{12}}{G_0} = (\dot{\gamma}\tau_0)\frac{\sqrt{1+8\beta(\dot{\gamma}\tau_0)^2}-1}{4\beta(\dot{\gamma}\tau_0)^2}$$

$$\frac{N_1}{G_0} = \frac{1}{\beta} + \frac{1}{4\beta(\dot{\gamma}\tau_0)^2} - \frac{\sqrt{1+8\beta(\dot{\gamma}\tau_0)^2}}{4\beta(\dot{\gamma}\tau_0)^2} \tag{19-20}$$

where G_0 is the plateau modulus, τ_0 is the relaxation time if there is no flow, and β is a changeable parameter (Marrucci and Ianniruberto, 1997).

CHAPTER IV

MATERIALS AND METHODOLOGY

4.1 Materials

4.1.1 Surfactant

Amidoamine oxide surfactant is a highly-active, biodegradable surfactant to be used as a gelling agent in brine and other aqueous solutions. With the addition of an aqueous brine solution (1-10 vol% brine), the surfactant will produce a viscoelastic gel. The gel has a low viscosity at higher shear rates, but at low shear rates, it has a high viscosity**.**

The amidoamine oxide gelling agent composition can generally be prepared by dissolving a tertiary amidoamine of general formula in a glycol solvent. The chemical structure is given by in **Fig. 13**;

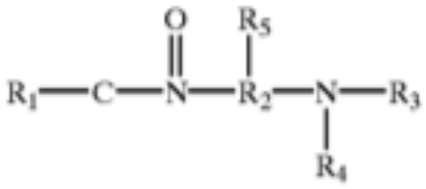

Fig. 13—The chemical structure of the surfactant.

where R_1 is a saturated or unsaturated, straight or branched chain aliphatic group of about 7 to 30 carbon atoms, R_2 is a divalent alkylene group of 2 to about 6 carbon atoms, R_3 and R_4 are the same or different, and are alkyl, or hydroxyalkyl of 1 to about 4 carbon

atoms. The suitable oxidation catalysts could be carbon dioxide, a carbon salt, a bicarbonate salt and mixtures (Hoey et al., 2003).

The composition of the surfactant and the physical and chemical properties are given in Table 1-2 (Akzo Nobel, 2010).

TABLE 1—COMPOSITION OF THE SURFACTANT

Name	% by Weight
Amides, tallow, n-[3 (dimethylamino)propyl], n-oxides	50-65
Propylene Glycol	25-40
Water	5-10

TABLE 2—PHYSICAL AND CHEMICAL PROPERTIES OF THE SURFACTANT

Property	Value
Physical State	Liquid
Appearance	Clear Yellow
Relative Vapor Density	2.62 (Air=1)
Viscosity (at 25°C and 10 s^{-1})	450 cp
Melting Point	4°C
Solubility	Soluble in water, methanol
Density (at 30°C)	0.99 g/cm^3

4.1.2 Brine Solutions

Calcium bromide and Calcium chloride brines were used in this study. Calcium bromide is the calcium salt of hydrobromic acid with the chemical formula of $CaBr_2$. Calcium chloride, $CaCl_2$, is a salt of calcium and chlorine. The composition and the physical and chemical properties of $CaBr_2$ (Chemtura, 2006) and $CaCl_2$ (Baker Hughes, 2011) are given in Tables 3-6.

TABLE 3—COMPOSITION OF CALCIUM BROMIDE SOLUTION

Name	% by Weight
Calcium Bromide	~54
Water	~46

TABLE 4—PHYSICAL AND CHEMICAL PROPERTIES OF $CaBr_2$

Property	Value
Physical State	Liquid
Appearance	Colorless water-white liquid
Solubility in Water	Miscible
Weight per Gallon	~14.2
Boiling Point	265°F
pH	6-8
Density (Water=1) (at 77°F)	1.7-1.73

TABLE 5—COMPOSITION OF CALCIUM CHLORIDE SOLUTION

Name	% by Weight
Calcium Chloride	~38
Water	~62

TABLE 6—PHYSICAL AND CHEMICAL PROPERTIES OF $CaCl_2$

Property	Value
Physical State	Liquid
Appearance	Clear
Specific Gravity	1.382
Weight per Gallon	~11.64
pH	5.72

4.1.3 Dispersant

Propylene Glycol (MPG), also called 1,2-propanediol or propane-1,2-diol, is an organic compound with formula $C_3H_8O_2$. It was used as a dispersant in the system. The physical and chemical properties of MPG is given in Table 7 (Fisher Scientific, 2009).

TABLE 7—PHYSICAL AND CHEMICAL PROPERTIES OF MPG

Property	Value
Physical State	Viscous Liquid
Appearance	Clear
Relative Vapor Density	2.62 (Air=1)
Viscosity (at 20°C)	45 mPa.s
Melting Point	-60°C
Molecular Weight	76.1
Molecular Formula	$C_3H_8O_2$
Solubility	Soluble in water
Specific Gravity (at 30°C)	1.03

4.1.4 Viscosity Stabilizers

MgO (Inframat Advanced Materials, 2009) and ZnO (Inframat Advanced Materials, 2008) nanoparticles have high surface area and were used as viscosity stabilizers in VES fluid systems at high temperatures. MgO microparticles are made from magnesium chloride brine and dolomitic lime (www.magnesiaspecialties.com). Table 8-10 shows the physical and chemical properties of these particles.

TABLE 8—PHYSICAL AND CHEMICAL PROPERTIES OF MgO NANOPARTICLES

Property	Value
Appearance	White Powder
Odor	Odorless
Vapor Density (at 20°C)	3.58 g/cm^3
Solubility in water (at 30°C)	0.86 g/l
Melting Point	2852°C

TABLE 9—PHYSICAL AND CHEMICAL PROPERTIES OF ZnO NANOPARTICLES

Property	Value
Appearance	White Powder
Odor	Odorless
Vapor Density (at 20°C)	5.6 g/cm^3
Solubility in water, %	Insoluble
Melting Point	1980°C

TABLE 10—PHYSICAL AND CHEMICAL PROPERTIES OF MgO MICROPARTICLES

Properties	Lower Specifications	Upper Specifications
Assay, % MgO	96	or greater
Loss on Ignition, %	Less than	8.5
CaO, %	Less than	2.0
Chloride (Cl), %	Less than	0.5
MAI, %	150	210
% Passing 325 Mesh	99.5	or greater
Median Particle Size, micron	Less than	3

4.1.5 Internal Breaker

The fish oil is obtained from fatty fish typically, anchovies, sardines, mackerel and herring. The oil contains a minimum of 18% EPA (eicosapentaenoic acid) and 12% DHA (docosahexaenoic acid) and a minimum of 35% total omega-3 (www.bioriginal.com)

4.2 Methodology

Apparent fluid viscosity was measured by using 4 vol% VES in 14.2 ppg $CaBr_2$ brine at 275°F and at 10 s^{-1}. Firstly, to prepare 4 vol% VES, 96 mL 14.2 ppg $CaBr_2$ was

put into a beaker and mixed in a stirrer. The 6 pptg (pound per 1000 gallon) 30 nm MgO nanoparticles were added to the fluid as a slurry in mono propylene glycol (MPG) using the ratio of 2.5 mL MPG per 1 g of particles. To prepare 6 pptg nanoparticles, 0.072 g MgO nanoparticles were weighed for 100 mL solution. The MPG and nanoparticles were mixed together for 3 minutes and then slurry was added to fluid to evenly disperse particles in fluid. This helped the particle dispersion within the fluid rather than staying as clumps. Then, 4 mL VES was added to this fluid and mixed in the stirrer at least 30 min. Once the particles were added to the fluid, the fluid should be tested within an hour. A testing error may occur if the sample was more than 1 or 2 hours old since the particles may try to interact and agglomerate once in the brine. The same procedure was applied to 4 vol% VES in 14.2 ppg $CaBr_2$ brine with 6 pptg 30 nm ZnO nanoparticles and without nanoparticles.

Another set of experiments was conducted by using 2 vol% VES in a 14.2 ppg $CaBr_2$ brine at 275°F and at 10 s^{-1}. To prepare 2 vol% VES, 98 mL 14.2 ppg $CaBr_2$ was put into beaker and mixed in the stirrer. The 6 pptg 30 nm MgO nanoparticles were added to the VES fluid as a slurry in mono propylene glycol (MPG) using the ratio of 2.5 mL MPG per 1 gram of particles and were mixed together for 3 minutes. Then, 2 mL VES was added to this fluid and mixed in the stirrer at least 30 min. The same procedure was applied to 2 vol% VES in 14.2 ppg $CaBr_2$ brine with 6 pptg 30 nm ZnO nanoparticles and without nanoparticles.

Apparent fluid viscosity was measured by using 4 vol% VES in 13 ppg $CaBr_2$ brine at 275°F and at 10 s^{-1}. Firstly, to prepare 13 ppg $CaBr_2$ brine solution, 79.5 mL

brine was put into the 100 mL volumetric flask and the distilled water was added until the total volume of the solution is 100 mL. Then, 96 mL 13 ppg $CaBr_2$ was put into a beaker and mixed in a stirrer. The 6 pptg (pound per 1000 gallon) 30 nm MgO nanoparticles were added to the VES fluid as a slurry in mono propylene glycol (MPG) using the ratio of 2.5 mL MPG per 1 gram of particles. The MPG and nanoparticles were mixed together for 3 minutes and 4 mL VES was added to this fluid and mixed in the stirrer at least 30 min. The same procedure was applied to 4 vol% VES in 13 ppg $CaBr_2$ brine with 6 pptg 30 nm ZnO nanoparticles and without nanoparticles.

Another set of experiments was conducted by using 4 vol% VES in 10.8 ppg $CaCl_2$ brine at 200°F and at 10 s^{-1}. Firstly, to prepare 10.8 ppg $CaCl_2$ brine solution, 75.5 mL brine was put into the 100 mL volumetric flask and the distilled water was added until the total volume of the solution is 100 mL. Then, 96 mL 10.8 ppg $CaCl_2$ was put into a beaker and mixed in a stirrer. The 6 pptg (pound per 1000 gallon) 30 nm MgO nanoparticles were added to the VES fluid as a slurry in MPG using the ratio of 2.5 mL MPG per 1 gram of particles and 4 mL VES was added to this fluid. The same procedure was applied to 4 vol% VES in 10.8 ppg $CaCl_2$ brine with 6 pptg 30 nm ZnO nanoparticles and without nanoparticles.

The aforementioned procedure to prepare 10.8 ppg $CaCl_2$ was performed. Then**,** 98 mL 10.8 ppg $CaCl_2$ was put into a beaker and mixed in a stirrer. The 6 pptg (pound per 1000 gallon) 30 nm MgO nanoparticles were added to the VES fluid as a slurry in MPG using the ratio of 2.5 mL MPG per 1 gram of particles. The MPG and nanoparticles were mixed together for 3 minutes and 2 mL VES was added to this fluid

and mixed in the stirrer at least 30 min. The same procedure was applied to 2 vol% VES in 10.8 ppg $CaCl_2$ brine with 6 pptg 30 nm ZnO nanoparticles and without nanoparticles.

To see the effect of different concentration of brine solutions, apparent fluid viscosity was measured by using 4 vol% VES in 11.6 ppg $CaCl_2$ brine at 180°F and at 10 s^{-1}. Firstly, to prepare 4 vol% VES, 96 mL 11.6 ppg $CaCl_2$ was put into a beaker and mixed in a stirrer. The 6 pptg (pound per 1000 gallon) 30 nm MgO nanoparticles were added to the VES fluid as a slurry in MPG using the ratio of 2.5 mL MPG per 1 gram of particles. Then, 4 mL VES was added to this fluid and mixed in the stirrer at least 30 min. The same procedure was applied to 4 vol% VES in 11.6 ppg $CaCl_2$ brine with 6 pptg 30 nm ZnO nanoparticles and without nanoparticles.

The effect of particle size was determined by using 4 vol% VES in 14.2 ppg $CaBr_2$ brine at 275°F with micro- and nano- MgO particles. The solution was prepared according to the method mentioned above. The 6 pptg (pound per 1000 gallon) MgO microparticles were added to the VES fluid as a slurry in mono propylene glycol (MPG) using the ratio of 2.5 mL MPG per 1 g of particles. The MPG and microparticles were mixed together for 3 minutes and then slurry was added to fluid to evenly disperse particles in fluid. Then, 4 mL VES was added to this fluid and mixed in the stirrer at least 30 min.

The effect of different particle concentration on the viscosity of VES micelles studied by using 4 vol% VES in 14.2 ppg $CaBr_2$ brine at 275°F and at 10 s^{-1}. The solution was prepared according to the method mentioned above. The 0.5, 2, 4, 6 and 8 pptg (pound per 1000 gallon) MgO nanoparticles were added to the VES fluid

respectively as a slurry in mono propylene glycol (MPG) using the ratio of 2.5 mL MPG per 1 g of particles. The MPG and nanoparticles were mixed together for 3 minutes and then slurry was added to fluid to evenly disperse particles in fluid. Then, 4 mL VES was added to this fluid and mixed in the stirrer at least 30 min, and then the apparent viscosity of each fluid system was measured.

4.2.1 Shear Rate Sweep

Shear rate sweep (100 to 1 s^{-1}) was performed for the 4 vol% VES in 14.2.ppg $CaBr_2$ brine from 100 to 250°F with and without MgO and ZnO nanoparticles. The sample was heated to 100°F and waited to shear at 100°F at 100 s^{-1} for 30 minutes, and then shear rate sweep was run. The same fluid was heated to 150°F and the same procedure was applied until 250°F.

4.2.2 Elasticity

Elasticity was measured in an HP/HT viscometer by using 4 vol% VES in 14.2 ppg $CaBr_2$ brine with and without MgO nanoparticles at 75°F and 275°F.

4.2.3 Internal Breaker

To break the VES micelles, a fish oil was used as an internal breaker, and apparent fluid viscosity was measured by using 4 vol% VES in 14.2 ppg $CaBr_2$ brine at 275°F and at 10 s^{-1}. Firstly, to prepare 4 vol% VES, 96 mL 14.2 ppg $CaBr_2$ was put into a beaker and mixed in a stirrer. The 6 pptg (pound per 1000 gallon) 30 nm MgO nanoparticles were

added to the VES fluid as a slurry in mono propylene glycol (MPG) using the ratio of 2.5 mL MPG per 1 g of particles. The MPG and nanoparticles were mixed together for 3 minutes and 1.5 gptg (gallon/1000 gallon) fish oil was added to the system. Then, with the addition of 4 mL VES to the fluid, the sample was mixed in the stirrer at least 30 min. The same procedure was applied by increasing the amount of fish oil from 1.5 to 3 gptg.

4.3 Equipment

4.3.1 An HP/HT Viscometer

An HP/HT viscometer was used to generate rheological data. This is a true Couette, coaxial cylinder, rotational, high pressure and temperature rheometer that works the pressure up to 1,000 psi and the temperature up to 500°F. Standard rotational testing measures the viscosity of the fluid, whereas oscillatory testing provides the capability to measure the elasticity of the fluid.

4.3.1.1 Procedure to Measure the Viscosity

To use this viscometer (**Fig.14**), the stress has to be between -10 and 10 dyn/cm^2. The sample cup is filled with fluid as 49 mL, and is installed by raising and screwing into place. The depressurization fitting on the bottom of the sample cup is tightened with a wrench and the oil bath is swung into position below the sample cup and lifted until covering the cup. The nitrogen supply valve is turned on to work at high temperature and the pressure increased. After this, the software program is set up by

entering the data such as the fluid temperature, shear rate, and step time.

Fig. 14—A high pressure/high temperature viscometer.

When the sample temperature decreases below 95°F, the nitrogen supply to the rheometer is turned off. A container is put below the sample cup to catch the sample when it is vented. The depressurization valve at the bottom of the sample cup is loosened with a wrench until the sample starts to flow from this point. When depressurization is completed, the sample cup is removed and the pressure regulator is set to 0 psi.

4.3.1.2 Procedure to Measure the Elasticity

To measure elasticity, the same procedure mentioned above is applied but there are three exceptions. Dynamic oscillatory testing has to be run instead of standard rotational testing and the volume of the sample has to be 68 mL. For viscosity measurements, the heavy Hastelloy C bob (Fig.15-a) is used but the hollowed one (Fig.15-b) is used for elasticity measurements.

Fig. 15—The heavy Hastelloy C (a) and hollowed (b) bob.

4.3.2 A Centrifuge

The centrifuge (**Fig.16**) was used to prevent air bubbles from being created when mixing the sample in a high speed, resulting in inaccurate rheometer measurements.

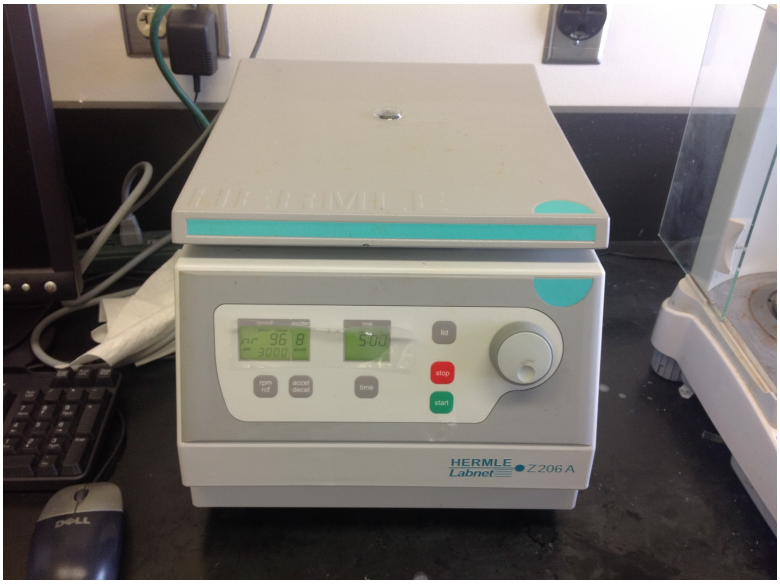

Fig. 16—The centrifuge.

4.3.2.1 Procedure

The weight of the tubes must be approximately the same and opposite each other. The speed can be chosen from the values between 200 to 6000 rpm and the running time can be selected in three different ranges from 10 seconds up to 99 hours 59 minutes. For this study, the speed is taken as 3000 rpm and the running time is set as 5 min. After the sample is placed, the centrifuge is started with manually selected parameters. When the running time has ended, the centrifuge stops automatically.

CHAPTER V

RESULTS AND DISCUSSION

The rheology of the amidoamine oxide surfactant in $CaBr_2$ and $CaCl_2$ brine solutions with and without nanoparticles were investigated in this study. VES fluids have very high viscosity at very low shear rates, making them a good choice for treating fluids such as fracturing fluids. Amidoamine oxide viscoelastic surfactants may provide more gelling power per pound, so these surfactants are less expensive than other fluids (Huang et al., 2011). The amount of VES fluid as a fracturing fluid may depend on two parameters: generating enough viscosity to control the rate of fluid leak off into the pores of the reservoir or fracture, and producing a high viscosity to fracture the formation during the hydraulic pumping. Therefore, depending on the application, about 0.5 to 25 vol% VES is added to the aqueous fluid and 2 to 4 vol% VES was used in this study (Huang et al., 2011). The formation of wormlike micelles depends on the change in the surfactant packing parameter by the addition of inorganic/organic salt (Israelachvili, 1992). Salts provide rapid micellar growth due to their strong binding to the micelles.

The stability of VES fluids may be enhanced by viscosity stabilizing agents. Viscosity stabilizing agents may cover alkali metal oxides, alkali metal hydroxides, alkali earth metal oxides, alkali earth metal hydroxides, transition metal oxides, transition metal hydroxides, glycols, and combinations. The particulate additives or stabilizing agents can be used at a temperature range from about 180 to 300°F

(Nettesheim et al., 2008). The increase in viscosity may be greatly variable, depending on parameters such as the type and amount of salinity, the type and concentration of VES, and the type and amount of additives (e.g. viscosity enhancers, internal breakers, defoamers, and gas hydrate inhibitors), impurities in the salts or brines used, rust or other metals that may contaminate the fluid during mixing. However, after preheating, the viscosity of VES gelled fluids will be higher than that before preheating (Huang et al., 2011). The viscosity stabilizers maintain VES fluid viscosity at high temperatures rather than increase the fluid viscosity. Viscosity stabilizers may have an average particle size of 500 nanometers or less, which leads to the stabilizer remaining with the VES fracturing fluid wherever it goes during the fracturing treatment and during flowback (Huang et al., 2011). The nanoparticles are added to monopropylene glycol to disperse within the fluid rather than staying as clumps.

The results from viscometer testing of the surfactant micellar fluids with and without nanoparticles are shown in **Fig. 17**. This shows the viscosities of VES fluids with and without nanoparticles at a temperature of 275°F and shear rate of 10 s^{-1}. With the addition of 6 pptg 30 nm MgO nanoparticles, the VES fluid system can maintain its viscosity at approximately 100 cp at 275°F. However, without nanoparticles, the viscosity decreases. In addition, MgO nanoparticles in 2 vol% VES in $CaBr_2$ brine fluid provide higher viscosity than ZnO nanoparticles in that fluid. Micelles in VES fluids may be spherical or wormlike and the transition from spherical to the wormlike micelles is caused by an increase in fluid viscosity (Huang et al., 2011).

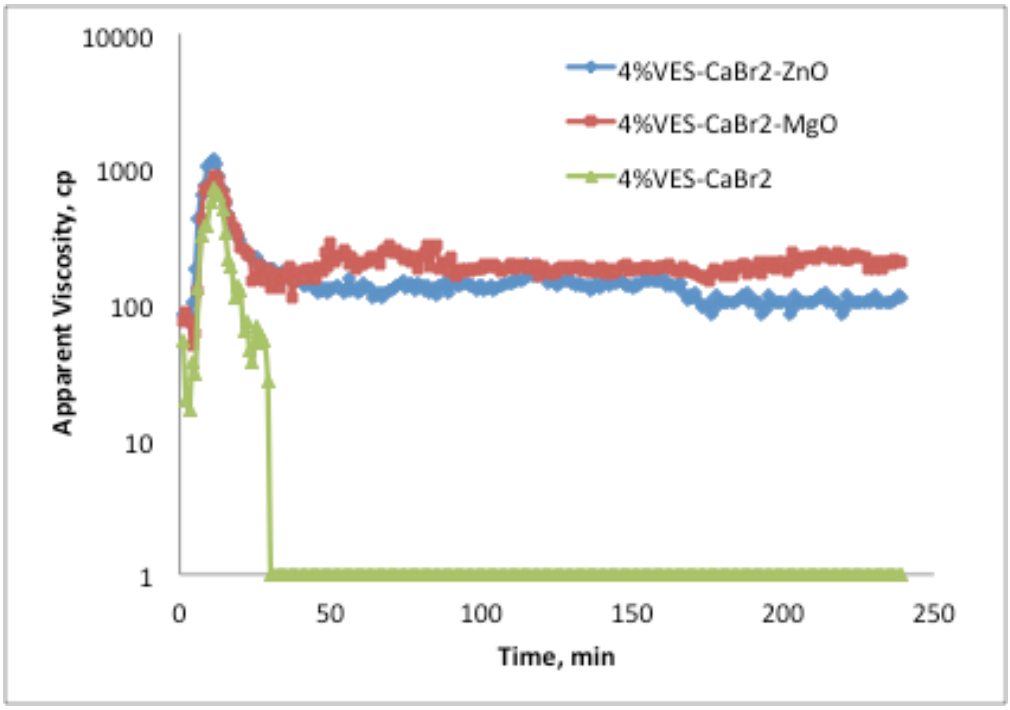

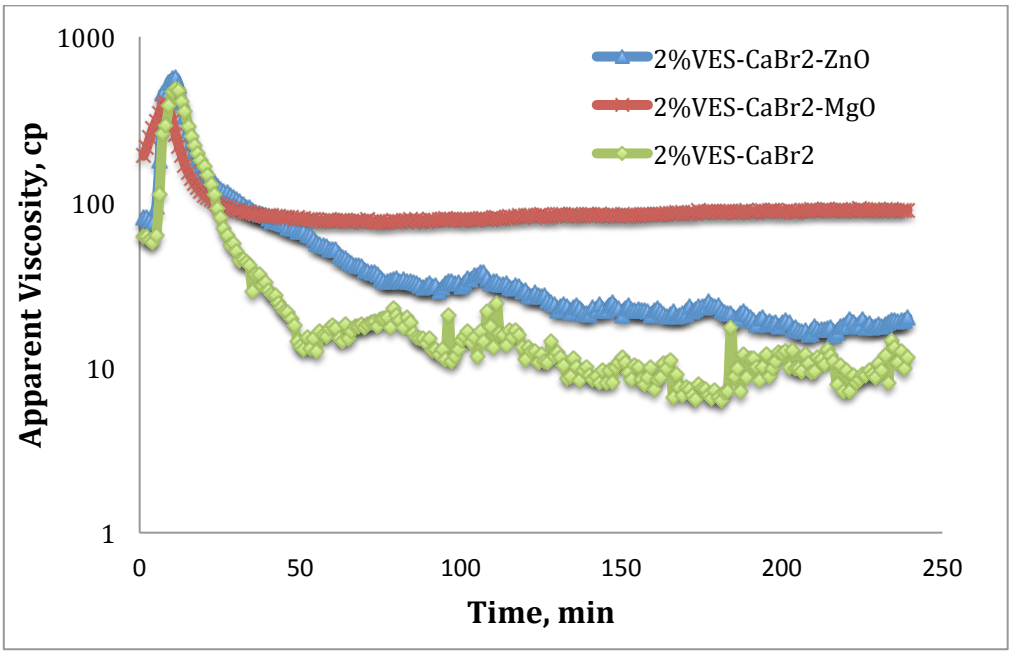

Fig. 17—The apparent viscosity of VES at concentrations of 4% (above) and 2% (below) shows that nanoparticles maintain the fluid's viscosity over time at 275°F, 10 s^{-1}.

VES micelles are not stable at high temperatures and thermally turn into nonviscous structures. The data indicates that the addition of nanoparticles increased and maintained viscosity at high temperatures. The increase in the viscosity of VES fluid is because of a change in the arrangement of surfactant molecules in the fluid. Viscoelasticity in the fluid arises from two separate mechanisms. The first is the entanglement of micelles, and the second is the micelle/particle junctions themselves, which effectively join two or more micelles, creating additional viscoelasticity (Helgeson et al., 2010). The comparison between 2 vol% and 4 vol% VES with and without nanoparticles at 275°F and a shear rate of 10 s^{-1} is shown in **Fig. 18**. An increase in the VES concentration leads to increase in the amount of micelle-to-micelle overlap and the viscosity of the fluid.

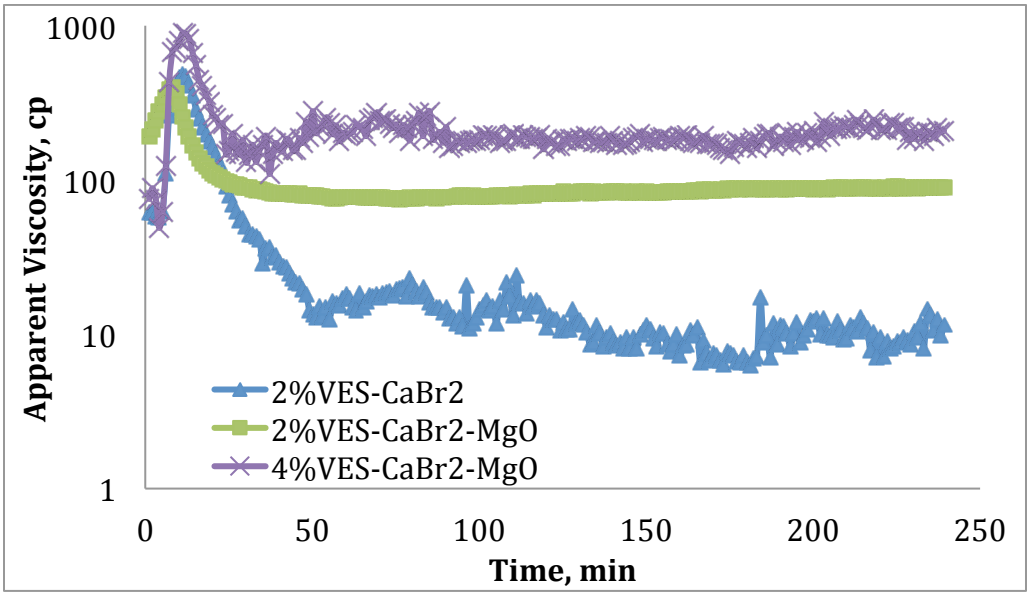

Fig. 18—When the surfactant concentration increases from 2 to 4 vol% VES, the viscosity of the fluid increases.

However at low surfactant concentrations (<8 mM), as the concentration of the surfactant is increased, more surfactant will adsorb on the surface of the particles and steric repulsive forces will increase in the system. This may affect the behavior of the system in two ways: decreasing the size and strength of the aggregates and contributing to partial stability in the system, which causes an overall decrease in the viscosity (Zaman et al., 2002).

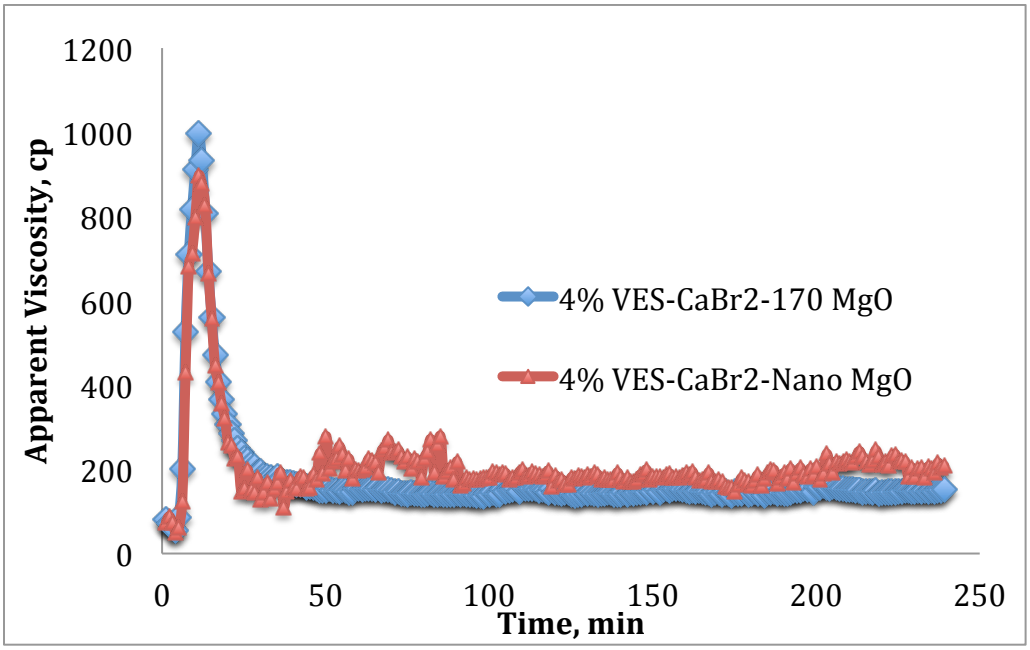

Fig. 19—The addition of micro- or nanoparticles to VES fluid maintains the viscosity at high temperatures and gives identical results.

Fig. 19 indicates that these micro- and nanoparticles give nearly identical results and help maintain the viscosity at 275°F. The MgO nanoparticles would stay within the VES that flows into the subterranean formation during a treatment. These

MgO nanoparticles may be used to stabilize the VES fluid instead of MgO microparticles for fluid-loss control treatments. The results from viscometer testing of the surfactant micellar fluids with and without nanoparticles at different shear rates and temperatures are shown in **Figs. 20-21**. This fluid contains 14.2 ppg $CaBr_2$ brine and 4 vol% VES at temperatures from 100 to 250°F and the shear rate from 100 to 1 s^{-1}, with 6 pptg MgO or ZnO nanoparticles. The low shear rate measurements were conducted after the fluids were static for 30 minutes at 100, 150, 200, and 250°F respectively. The addition of approximately 30 nm size particles to VES micellar fluids has shown improved viscosity yield at moderate, low, and ultralow fluid shear rates.

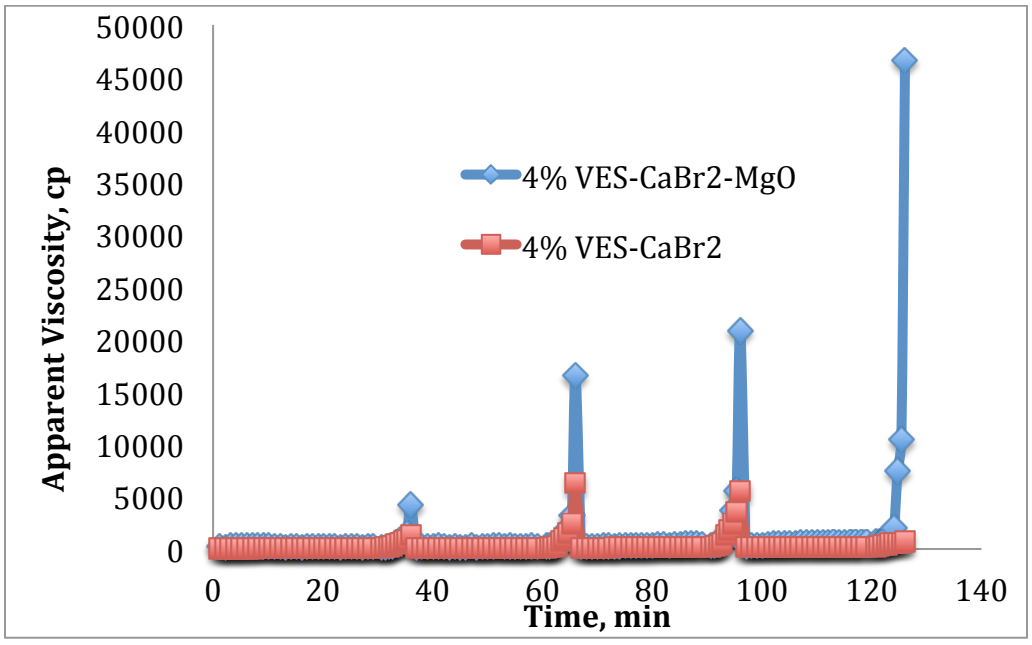

Fig. 20—When the temperature increases from 100 to 250°F and shear rate changes from 100 to 1 s^{-1}, the viscosity increases with the addition of nanoparticles.

Low shear rate tests proved about two-fold increase in fluid viscosity by the addition of nanoparticles. The increase by the addition of MgO nanoparticles is higher than that by the addition of ZnO nanoparticles.

When the temperature increases, the original bound charges will be released and distributed on the surface of nanoparticles. These surface-charged nanoparticles are absorbed on the wormlike micelle surface more easily and cause electrostatic screening of charged micelles. This can trigger micelle entanglement and formation of the more stable cross-linking network. On the other hand, the nanoparticle may absorb on the micelle end-cap and the micelle can generate a micelle–nanoparticle stalk.

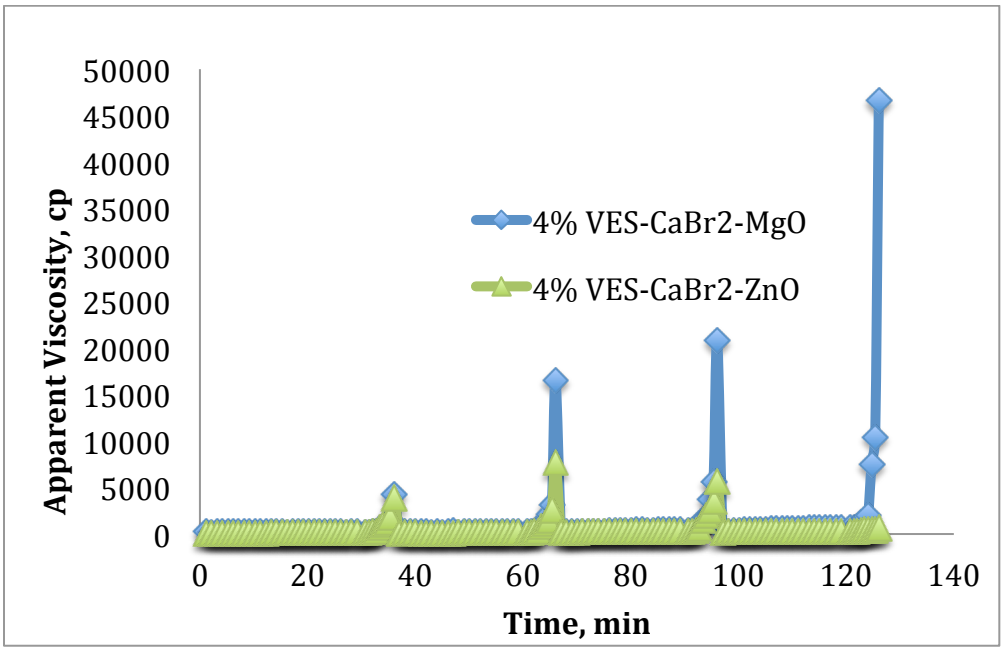

Fig. 21—The comparison of VES fluid system with MgO and ZnO nanoparticles at temperatures from 100 to 250°F and shear rates from 100 to 1 s^{-1}.

A single nanoparticle can hold many stalks in a liquid–solid interface and act as a junction of micelles because the surface area of the charged nanoparticle is much larger than the projected cross-section of the micelle. These nanoparticles with several junctions will incorporate into the micelle network and can maintain the network stability.If the temperature is higher than the critical value, the viscosity decreases with the increase of temperature, resulting in the breaking of micelle network because the outer energy is greater than the association energy between micelle and nanoparticle (Luo et al., 2012; Helgeson et al., 2010).

In **Fig. 22**, when the concentration of $CaBr_2$ is decreased from 14.2 ppg to 13 ppg, the loading of nanoparticles to VES micelles maintains the viscosity at 200 cp, but without nanoparticles the viscosity is less than 100 cp at 275°F.

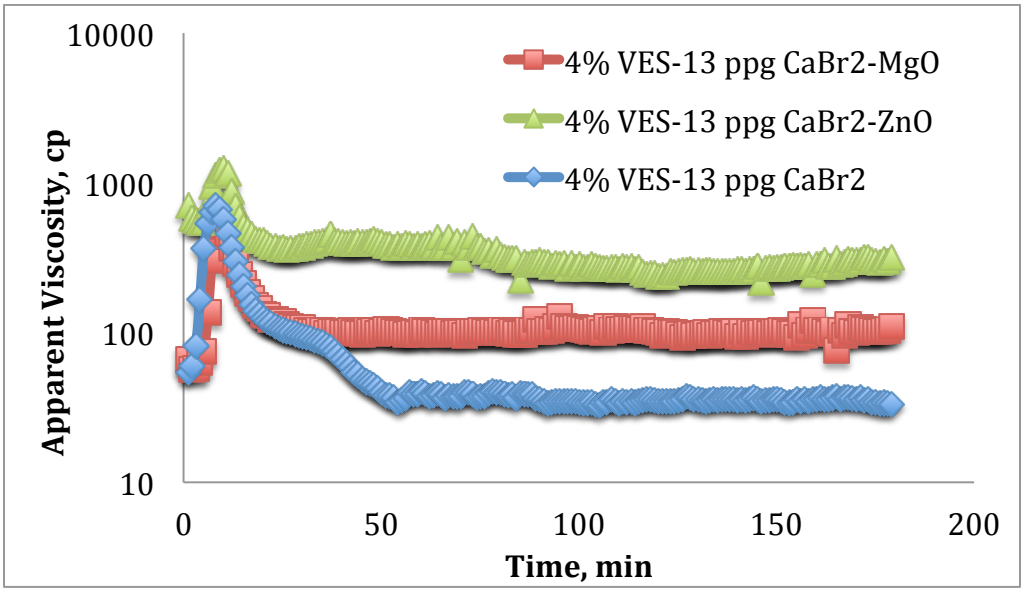

Fig. 22—When the salt concentration decreases, the VES micelles have viscosity stability at high temperatures.

The viscosities of 2 vol% and 4 vol% VES in 10.8 ppg $CaCl_2$ brine with and without nanoparticles at 200°F and a shear rate of 10 s^{-1} have been shown in **Fig. 23** and **Fig. 24**. The addition of approximately 30 nm MgO particles stabilizes the VES micelles, and VES micelles without nanoparticles have a 200 cp viscosity but the viscosity appears to decrease over time. For 4 vol% VES micelles, the viscosity without nanoparticles is a bit higher than that with either MgO or ZnO nanoparticles within 4 hours. These figures show that MgO particles/surfactant interaction generates a stronger network that causes increase in the viscosity more than ZnO particle/surfactant interaction.

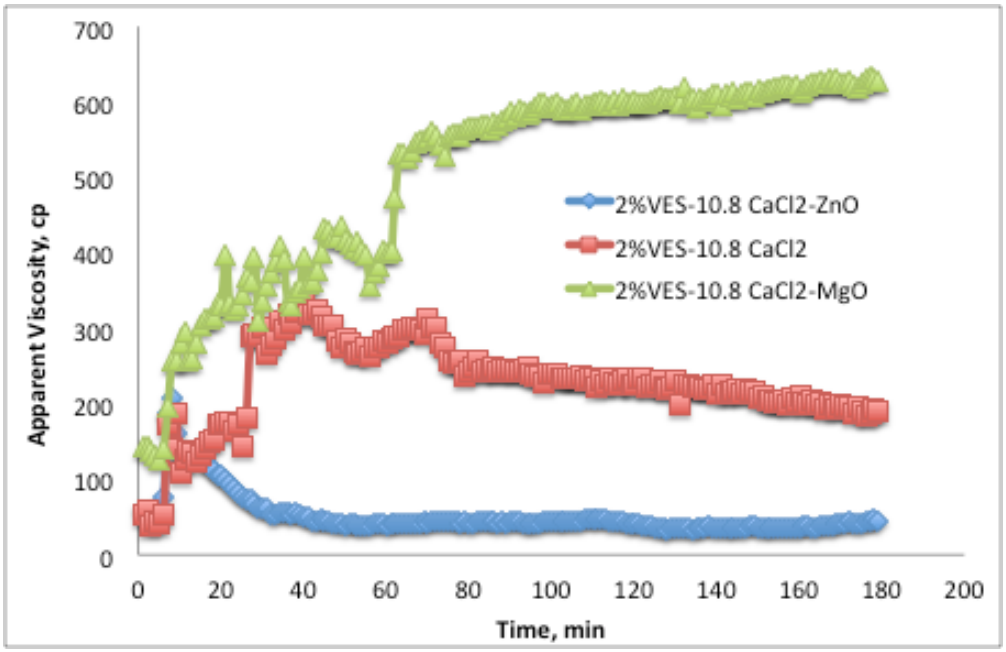

Fig. 23— The apparent viscosity of 2 vol% VES micelles in a 10.8 ppg $CaCl_2$ brine with and without nanoparticles.

The increase in the amount of salt causes an increase in the curvature energy of the surfactant molecules in the end caps. This results in an increase in micelle length, and the viscosity, forming an entangled network. However, the addition of large amounts of salt reduces the viscosity of VES micelles generated both by the entanglement of the wormlike micelles and by the electrostatic forces between micelles. This leads to the screening of the electrostatic interactions of the wormlike micelles and reduction in the effective head-group area (Van Zanten, 2011). There is no repulsion generated by the charged surfaces of the micelles, so the viscosity decreases. (Massiera et al. 2002; Massiera et al., 2003). According to the Hofmeister series, the relative influence of ions on the physical behavior of colloidal systems ranks as: $Br^- > Cl^-$.

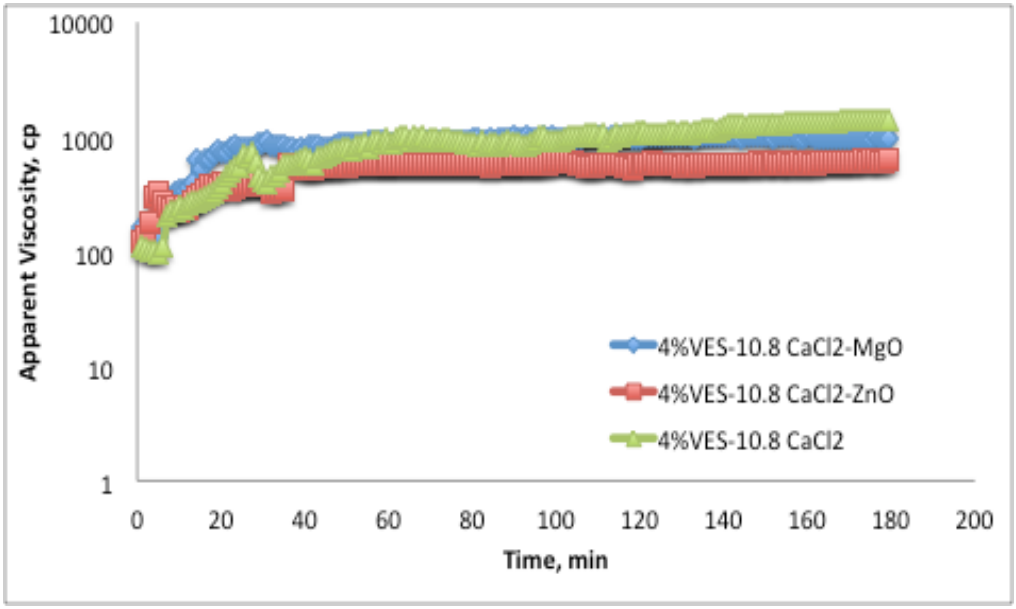

Fig. 24—The viscosity depends on the type of the salt solution and the concentration of surfactants.

The larger anions increase the adsorption of surfactants (Zhang and Cremer, 2006; Goodwin, 2009). Therefore, $CaBr_2$ seems more effective to interact with VES than $CaCl_2$ brine solutions.

Fig. 25 depicts the viscosity of 4 vol% VES in 11.6 ppg $CaCl_2$ brine with and without nanoparticles as a function of time. The VES micelles have some stability with and without nanoparticles.

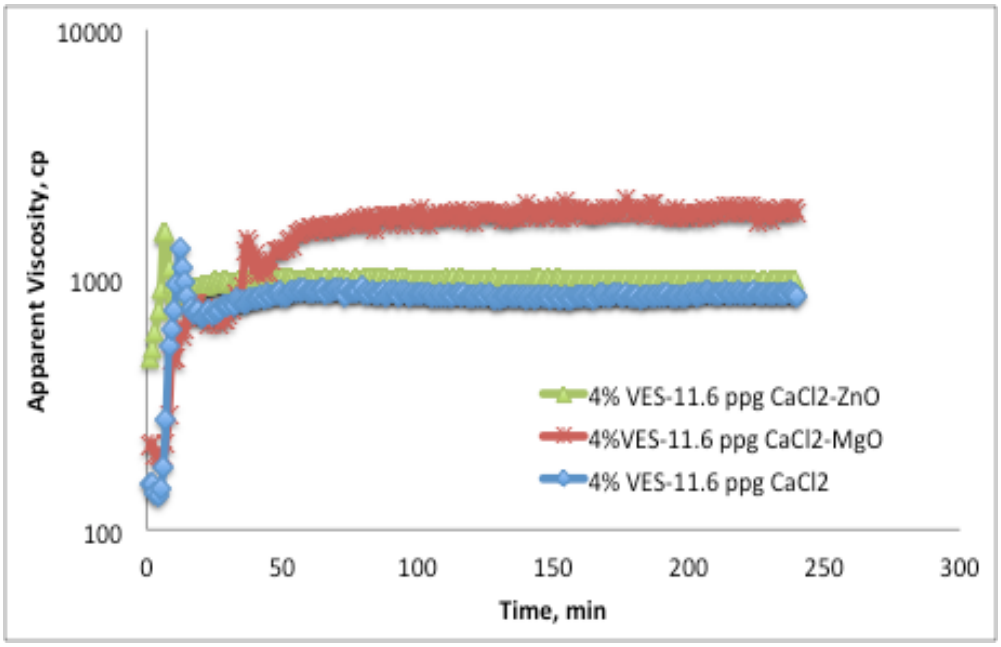

Fig. 25—The addition of MgO nanoparticles stabilizes the viscosity of VES micelles at 180°F.

However, the addition of ZnO or MgO nanoparticles to VES micelles may reduce viscosity to lower levels than VES micelles without nanoparticles. Luo et al., (2012) have suggested that the decrease in viscosity at high salt concentration may be

because of the formation of branched wormlike micelles. The crosslinks in the micelle network can slide along the micelles and therefore serve as stress release points. This branched micelle network will show a reduced viscosity compared to that of the entangled linear micelles. The nanoparticles at these conditions slightly promote the branching process.

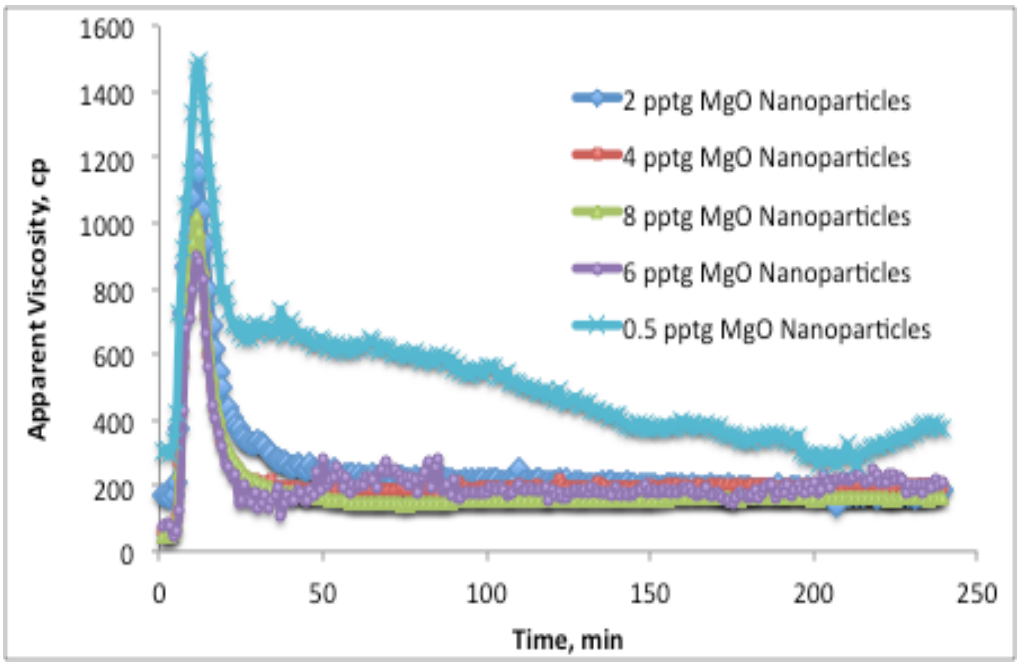

Fig. 26—The addition of different concentrations (2-8 pptg) of MgO nanoparticles gives identical results at 275°F.

The viscosities of 4 vol% VES in 14.2 ppg $CaCl_2$ brine with different particle concentration at 275°F and a shear rate of 10 s^{-1} have been shown in **Fig. 26.** The addition of nanoparticles should cause an increase in nonlinear viscosity with increasing particle concentration, and a decrease in the viscosity exponent in the overlap regime.

However, the viscosity of VES micelles at different concentrations gives approximately identical results except VES micelles with 0.5 pptg MgO nanoparticles, so this is independent of particle concentration.

The formation of micelle-nanoparticle junctions leads to the formation of crosslinked micellar aggregates in solution at WLM-nanoparticle mixtures below critical micelle concentration. Therefore, each nanoparticle will behave as an object with a larger effective hydrodynamic radius and the effective volume fraction of the suspended particles will be greater than the solid volume fraction of nanoparticles, which will cause the increase in viscosity. The synergistic effect of increasing both the salt and nanoparticle concentration for solutions is due to the fact that above the critical concentration, micellar junctions will generate a more considerable increase in the viscosity because of double network formation. Both parameters result in nonlinear increases in the effective reptation time (Helgeson et al., 2010).

Elasticity measurements were conducted with oscillatory testing in the HP/HT viscometer. The results from the measurements are seen in these figures from **Figs. 27-30**. Storage and loss modulus of 4 vol% VES in 14.2 ppg $CaBr_2$ at 75°F are plotted as a function of time in **Fig. 27**. The dominant factor is storage modulus at room temperature and loss modulus is dominant at high temperature as seen in **Fig. 28**.

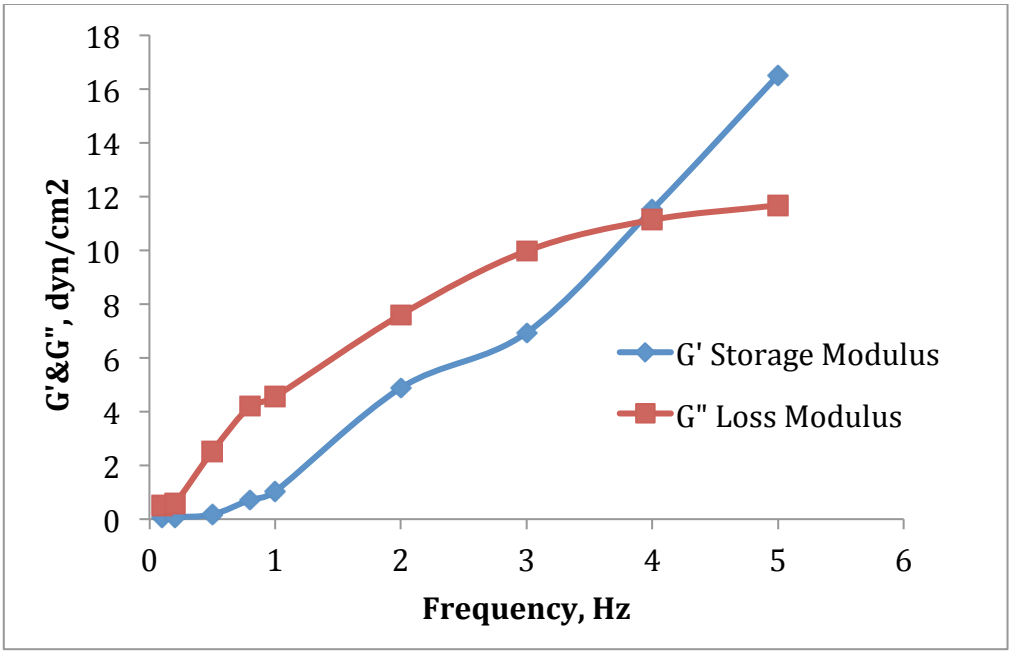

Fig. 27—Storage modulus is the dominant factor for VES fluid system without nanoparticles at room temperature.

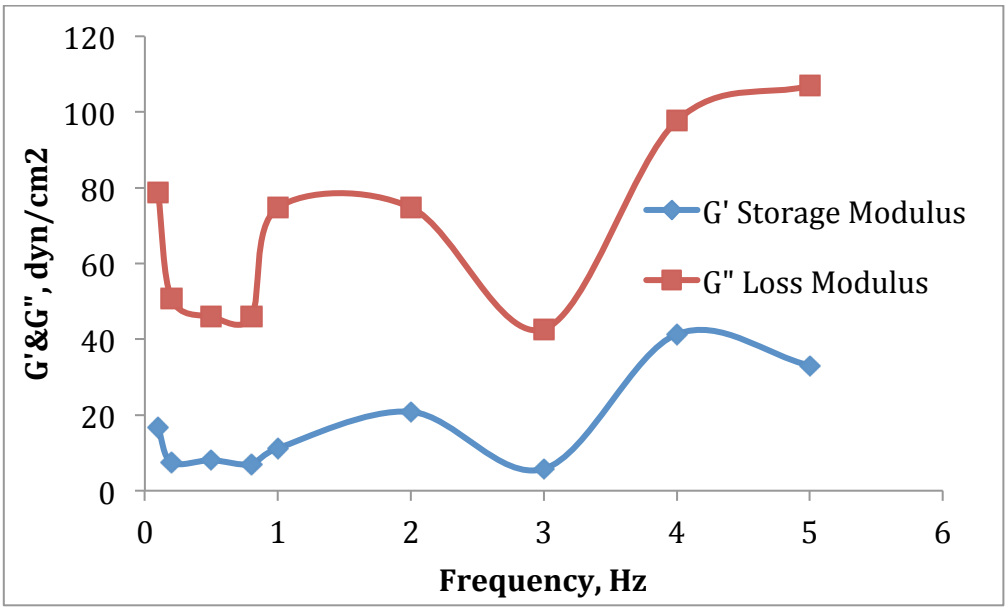

Fig. 28—Loss modulus is the dominant factor for VES fluid system without nanoparticles at 275°F.

When the nanoparticles are added to the system at room temperature and 275°F, the loss modulus becomes the dominant factor, and the curve shows a maximum and then a decrease, as seen in **Figs. 29-30**. At a critical frequency, the response of the dispersion changes from viscous to elastic behavior. The moduli for the samples containing 4 vol% VES in a 14.2 ppg $CaBr_2$ brine are strongly frequency dependent.

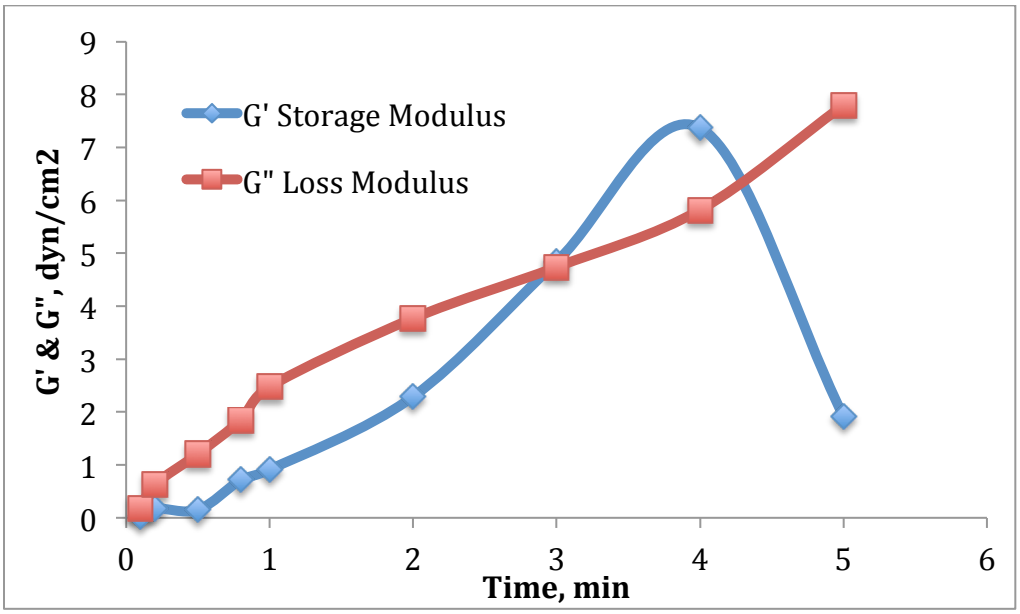

Fig. 29—Loss modulus is the dominant factor for VES fluid system with MgO nanoparticles at room temperature.

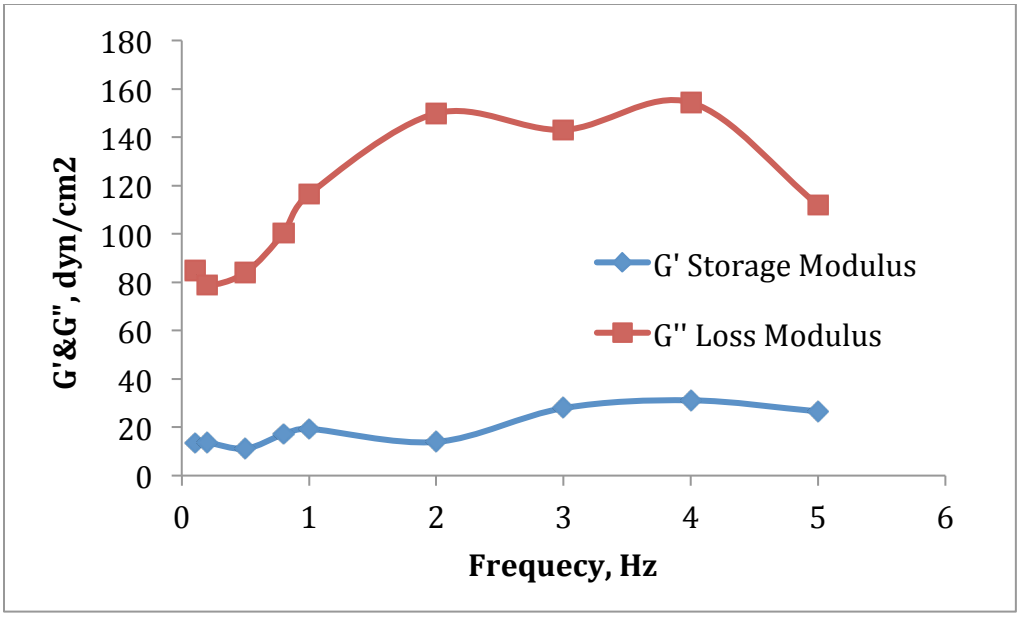

Fig. 30—Loss modulus is the dominant factor when the nanoparticles are added to VES fluid system at 275°F.

The storage modulus G′ depicts the energy storage in the structure of the VES fluid and is related to strength of the flocculated network. The decrease in the value of the G′ means the weakening of the network structure resulted from the formation of micelle-like spherical aggregates on the surface of the particles. Therefore, viscous forces will consume most of the energy and the amount of energy stored may be negligible. The dominance of elastic modulus indicated that the micelles were strongly networked (Zaman et al., 2002).

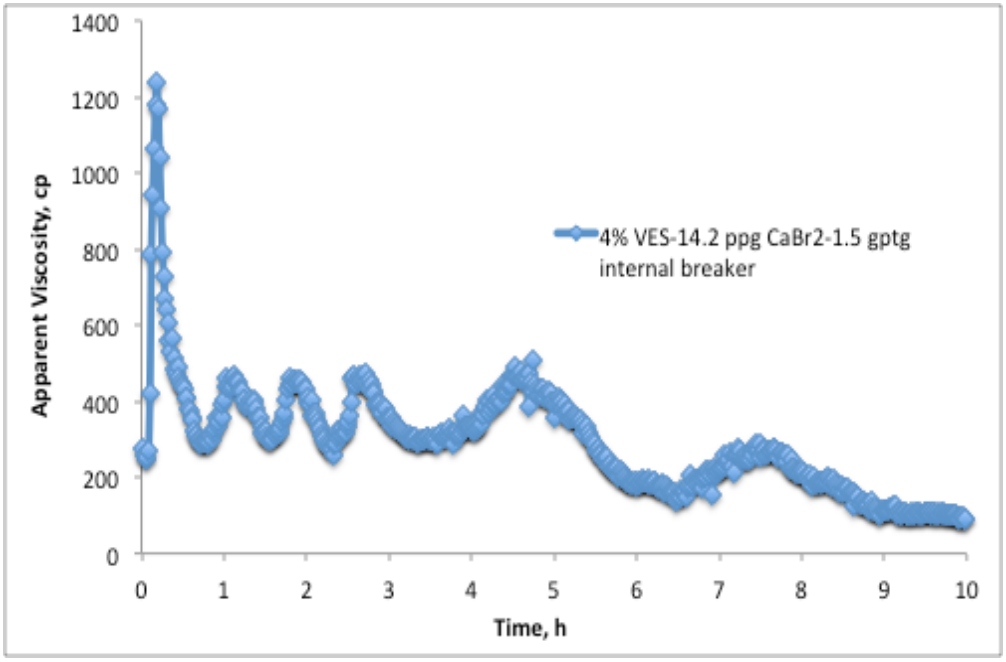

Fig. 31—The breaking of VES micelles with 1.5 gptg internal breaker at 275°F.

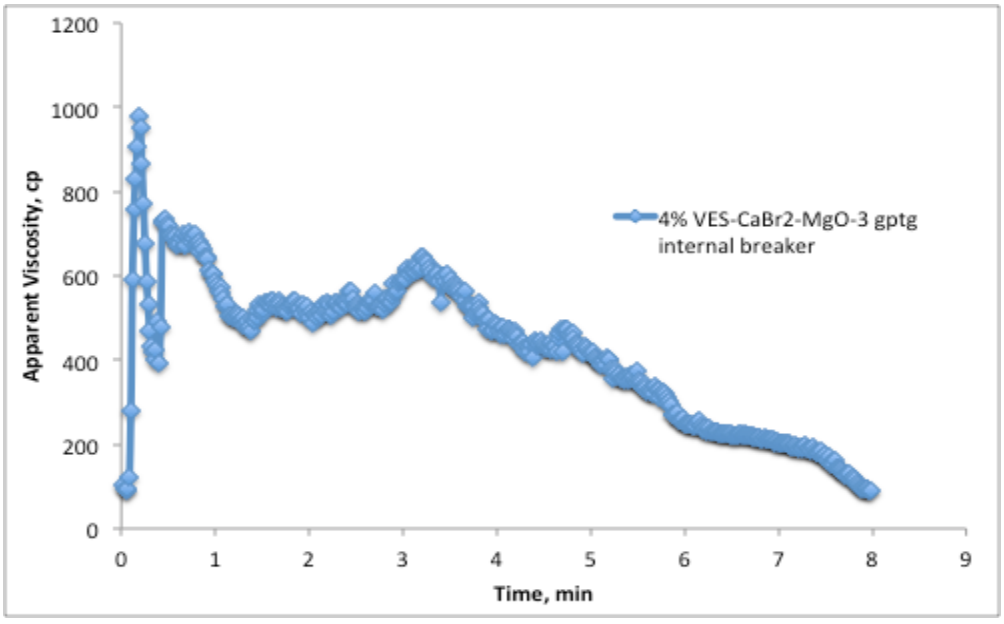

Fig. 32—The breaking of VES micelles with 3 gptg internal breaker at 275°F.

The application of internal breaker at 275°F is shown in **Figs. 31-32.** The fluid system used was 4 vol% VES in 14.2 ppg $CaBr_2$ brine with MgO nanoparticles and 1.5 gptg internal breaker. The fish oil was used as an internal breaker. The breaker systems will turn wormlike VES micelles into non-viscous, more spherical micelles by generating VES breaking compounds over time (Crews et al., 2008). The apparent viscosity as a function of time data shows that the viscosity reduces rapidly with higher breaker loadings. When the internal breakers break the VES micelles that generate pseudo-filter cake, the filter cake will collapse into broken VES fluid with nanoparticles (Huang and Crews, 2008).

CHAPTER VI

CONCLUSIONS AND RECOMMENDATIONS

6.1 Conclusions

In this work, the amidoamine oxide surfactant in $CaBr_2$ or $CaCl_2$ brine solutions with MgO or ZnO nanoparticles and fish oil as an internal breaker were used. The results indicate that a considerable strengthening of micellar entanglements and the increase in viscosity of VES fluid can be induced by the addition of a small amount of nanoparticles. The conclusions of this work are as follows:

1) The addition of 6 pptg MgO or ZnO nanoparticles to the VES fluid system maintains the viscosity at 275°F. However, without nanoparticles, the viscosity decreases at this temperature. In addition, MgO nanoparticles in 2 vol% VES in 14.2 ppg $CaBr_2$ brine fluid provide higher viscosity than ZnO nanoparticles in that fluid.

2) An increase in the VES concentration from 2 to 4 vol% leads to increase in the amount of micelle-to-micelle overlap and the viscosity of the fluid.

3) Micro- and nanoparticles have potential to improve viscosity of VES fluids; similarly, but nanoparticles may be the better choice for fluid loss control. The MgO nanoparticles would stay within the VES that flows into the subterranean formation during a treatment.

4) The addition of approximately 30-nm particles to VES micellar fluids has showed improved viscosity yield at moderate, low, and ultralow fluid shear rates. Low shear rate tests proved about two-fold increase in fluid viscosity by the addition of

nanoparticles. The increase by the addition of MgO nanoparticles is higher than that by the addition of ZnO nanoparticles.

5) When the salt concentration is decreased from 14.2 ppg to 13 ppg, the VES micelles with nanoparticles has some viscosity stability. The increase in the amount of salt causes an increase in the curvature energy of the surfactant molecules in the end caps, and the viscosity of VES micelles. However, the addition of large amounts of salt causes the decrease in the viscosity of VES micelles generated both by the entanglement of the wormlike micelles and by the electrostatic forces between micelles.

6) The viscosity of VES micelles at different concentrations has approximately identical results except VES micelles with 0.5 pptg MgO nanoparticles, so this is independent of particle concentration.

7) For VES micellar systems without nanoparticles, the dominant factor is storage modulus at room temperature and loss modulus becomes dominant at high temperature. When the nanoparticles are added to the system at 275°F, the loss modulus becomes the dominant factor.

8) The apparent viscosity of 4 vol% VES in 14.2 ppg $CaBr_2$ brine with MgO nanoparticles reduces rapidly with the loading of 1.5 gptg internal breaker. The breaker systems turn wormlike VES micelles into non-viscous micelles.

6.2 Recommendations

In this work, the amidoamine oxide surfactant in a brine solution with and without nanoparticles was investigated, but the topic should be further analyzed both experimentally and theoretically for a better understanding. The mechanism of nanoparticle/surfactant interaction has still not been completely understood. Different types and amounts of surfactants and brine solutions can be used to see their effect on the viscosity of threadlike micelles. The optimization of the addition of nanoparticles can be studied at high temperatures for fluid loss control. The economic analysis of this system can be studied to investigate whether it is economically feasible or not. The dynamics of colloidal particles should be quantified using Diffusing-Wave Spectroscopy (DWS) and a micro rheological approach in order to understand the interactions between particles and micelles.

REFERENCES

Adler, J.J., Singh, P.K., Patist, A., et al. 2000. Correlation of Particulate Dispersion Stability with the Strength of Self-Assembled Surfactant Films. Langmuir, 16, 7255-7262.

Berret, J.F. 2004. Rheology of Wormlike Micelles: Equilibrium Properties and Shear Banding Transition. Molecular Gels: Materials With Self-assembled Fibrillar Networks, Springer, Netherlands.

Berret, J.F., Roux, D.J., and Lindler, P. 1998. Structure and Rheology of Concentrated Wormlike Micelles at the Shear-induced Isotropic-to-nematic Transition. Phys. J.B 5, 67.

Bioriginal Complete & Innovative EFA Solutions. 2012. http://www.bioriginal.com/products/ (accessed 10 August 2012).

Cates, M.E. 1990. Non-linear viscoelasticity in wormlike micelles (and other reversibly breakable polymers). J.Phys. Chem. 94, 371.

Cates, M.E., Fielding, S.M., 2006. Rheology of giant micelles. Adv. Phys. 55, 799–879.

Crews, J.B. 2005. Internal Phase Breaker Technology for Viscoelastic Surfactant Gelled Fluids. Paper presented at the SPE International Symposium on Oilfield Chemistry, The Woodlands, TX. SPE-00093449. DOI: 10.2118/93449-ms.

Crews, J.B. and Gomaa, A.M. 2012. Nanoparticle Associated Surfactant Micellar Fluids: An Alternative to Crosslinked Polymer Systems. Paper presented at the SPE International Oilfield Nanotechnology Conference, Noordwijk, The Netherlands. SPE-157055-MS. DOI: 10.2118/157055-ms.

Crews, J.B. and Huang, T. 2007. Internal Breakers for Viscoelastic-Surfactant Fracturing Fluids. Paper presented at the International Symposium on Oilfield Chemistry, Houston, TX. SPE-106216-MS. DOI: 10.2118/106216-ms.

Crews, J.B. and Huang, T. 2008. Use of Nano-Sized Clay Minerals in Viscoelastic Surfactant Fluids. US 2008/0300153.

Crews, J.B. and Huang, T. 2011. Re-Use of Surfactant-Containing Fluids. US WO 2011/084776.

Crews, J.B., Huang, T., Gabrysch, A., Evans, B. 2010. Nanoparticle Networked Surfactant Micellar Fluids-Completion Fluids with Reduced Formation Damage. Paper presented at the 2010 AADE Fluids Conference and Exhibition, Houston, Texas, USA. AADE-10-DF-HO-02.

Crews, J.B., Huang, T., and Wood, W.R. 2006. New Fluid Technology Improves Performance and Provides a Method to Treat High-Pressure and Deepwater Wells. Paper presented at the SPE Annual Technical Conference and Exhibition, San Antonio, Texas, USA. SPE-103118-MS. DOI: 10.2118/103118-ms.

Crews, J.B., Huang, T., and Wood, W.R. 2008. New Technology Improves Performance of Viscoelastic Surfactant Fluids. SPE Drilling & Completion 23 (1): 41-47. DOI: 10.2118/103118-pa.

Fischer, P., Rehage, H., Grüning, B. 1994. Rheological Properties of Dimeric Acid Betaine Solutions, Tenside Surf. Det. 31, 99 - 108.

Fischer, P., Rehage, H., Grüning, B. 2002. Linear Flow Properties of Dimer Acid Betaine Solutions with and without Changed Ionic Strength, J. Phys. Chem. B 106, 11041-11046.

Goodwin, J.W. 2009. Colloids and Interfaces with Surfactants and Polymers. West Sussex, UK: Wiley & Sons Ltd.

Goodwin, J.W. and Hughes, R.W. 2008. Rheology for Chemists: An Introduction. Cambridge, UK: The Royal Society of Chemistry.

Gogarty, W.B. 1974. Use of Viscoelastic Fluids For Mobility Control. USA. 3822746.

Graduate, Lu, S. 2008. Nanostructures of mixed surfactant aggregates: Adsorption, solubilization and viscoelasticity. PhD dissertation. New York City, New York, USA: Columbia University.

Grand, C., Arrault, J., and Cates, M.E. 1997. Slow Transients and metastability in wormlike micelle rheology. J. Phys. II France 7, 1071.

Gupta, D. V. S. 2009. Unconventional Fracturing Fluids for Tight Gas Reservoirs. Paper SPE 119424 presented at the SPE Hydraulic Fracturing Technology Conference, Houston, Texas.

Helgeson, M.E., Hodgdon, T.K., Kaler, E.W. et al. 2010. Formation and Rheology of Viscoelastic “Double Networks” in Wormlike Micelle−Nanoparticle Mixtures. Langmuir 26 (11): 8049-8060. DOI: 10.1021/la100026d.

Hoey, M.D., Franklin, R., Lucas, D.M., et al. 2003. Viscoelastic Surfactants and Compositions Containing Same. US 6506710.

Holmberg, K., Jönsson, B., and Kronberg, B., et al. 2003. Surfactants and Polymers In Aqueous Solution. West Sussex, UK: John Wiley & Sons Ltd.

Huang, T. 2008. Viscosity Enhancers For Viscoleastic Surfactant Stimulation Fluids. US 2008/0139419.

Huang, T., Crews, J.B. 2007. Nanotechnology Applications in Viscoelastic Surfactant Stimulation Fluids. Paper presented at the European Formation Damage Conference, Scheveningen, The Netherlands. SPE-107728-MS. DOI: 10.2118/107728-ms.

Huang, T. and Crews, J.B. 2008a. Do Viscoelastic-Surfactant Diverting Fluids for Acid Treatments Need Internal Breakers? Paper presented at the SPE International Symposium and Exhibition on Formation Damage Control, Lafayette, Louisiana, USA. SPE-112484-MS. DOI: 10.2118/112484-ms.

Huang, T. and Crews, J.B. 2008b. Nanotechnology Applications in Viscoelastic Surfactant Stimulation Fluids. SPE Production & Operations 23 (4): 512-517. DOI: 10.2118/107728-pa.

Huang, T. and Crews, J.B. 2008c. Solids Suspension with Nanoparticle-Associated Viscoelastic Surfactant Micellar Fluids. US 2008/0153720.

Huang, T., Crews, J.B., and Agrawal, G. 2010. Nanoparticle Pseudocrosslinked Micellar Fluids: Optimal Solution for Fluid-Loss Control with Internal Breaking. Paper presented at the SPE International Symposium and Exhibiton on Formation Damage Control, Lafayette, Louisiana, USA. SPE-128067-MS. DOI: 10.2118/128067-ms.

Huang, T., Crews, J.B., and Willingham, J.R. 2008. Nanoparticles for Formation Fines Fixation and Improving Performance of Surfactant Structure Fluids. Paper presented at the International Petroleum Technology Conference, Kuala Lumpur, Malaysia. International Petroleum Technology Conference IPTC-12414-MS. DOI: 10.2523/12414-ms.

Huang, T., Crews, J.B. and Willingham, J.R. 2009. Multifunctional Nanoparticles For Downhole Formation Treatments. US 0065209.

Huang, T., Crews, J.B., and Willingham, J.R. 2011. Methods of Using Viscoelastic Surfactant Gelled Fluids To Pre-Saturate Underground Formations. US 8056630.

Hunter, T.N., Pugh, R.J., Franks, G.V. et al. 2008. The Role of Particles in Stabilising Foams and Emulsions. Advances in Colloid and Interface Science 137: 57-81. DOI: 10.1016/j.cis.2007.07.007.

Hunter, T.N., Wanless, E.J., Jameson, G.J. et al. 2009. Non-Ionic Surfactant Interactions with Hydrophobic Nanoparticles: Impact on Foam Stability. Colloids and Surfaces A: Physicochemical and Engineering Aspects 347 (1–3): 81-89. DOI: 10.1016/j.colsurfa.2008.12.027.

In, M. 2001. Reactions and Synthesis in Surfactant Systems. New York, Marcel Dekker Inc.

In, M., Aguerre-Chariol, O., Zana, R. 1999. Closed-Looped Micelles in Surfactant Tetramer Solutions, J. Phys. Chem. B 103, 7747 – 7750.

Israelachvili, J.N. 1992. Intermolecular and surface forces. Academic Press, London.

Israelachvili, J.N., Mitchell, D.J. 1975. Biochimica Et Biophysica Acta, 389. 1. 13-19.

Israelachvili, J.N., Mitchell, D.J., Ninham, B.W., 1976. J.Chem. Soc. Faraday Trans. 2. 72. 1525.

Kahlweit, M. 1985. In Physics of Amphiphiles, Micelles, Vesicles and Microemulsions, Degiorgio, V., Corti, M., Eds., North-Holland, Amsterdam.

Kaler, E.W., Herrington, K.L., Murthy, A.K., et al. 1992. Phase Behavior and Structures of Mixtures in Anionic and Cationic Surfactants, J. Phys. Chem. 96, 6698–6707.

Koehler, R.D., Raghavan, S.R., Kaler, E.W. 2000. Microstructure and Dynamics of Wormlike Micellar Solutions Formed by Mixing Cationic and Anionic Surfactants, J. Phys. Chem. B 104, 11035–11044.

Larson, R.G. 1999. Rheology of Complex Fluids, Oxford University Press.

Leitzell, J.R. 2007. Viscoelastic Surfactants: A New Horizon in Fracturing Fluids for Pennsylvania. Paper presented at the Eastern Regional Meeting, Lexington, Kentucky USA. SPE-111182-MS. DOI: 10.2118/111182-ms.

Lequeux, F., Candau, S.J. 1994. Structure and Flow in Surfactant Solutions (ACS Symposium Series 578), Washington D.C., American Chemical Society.

Lessner, E., Teubner, M., Kahlweit, M. J., 1981. Phys. Chem. 85. 3167.

Luo, M., Jia, Z., Sun, H. et al. 2012. Rheological Behavior and Microstructure of an Anionic Surfactant Micelle Solution with Pyroelectric Nanoparticle. Colloids and Surfaces A: Physicochemical and Engineering Aspects 395: 267-275.

Magnesium Oxide Powder. MSDS. Inframat Advanced Materials, LLC: Manchester, CT. August, 2009.

Marrucci, G. 1996. Dynamics of Entanglements: A non-linear model consistent with the Cox-Merz rule. J. Non-Newtonian Fluid Mech. 62, 279.

Martin Marietta Magnesia Specialties. 2010. http://www.magnesiaspecialties.com/mc_rubber_plastics.htm (accessed 10 August 2012).

Marucci, G., and Ianniruberto, G. 1997. Effect of flow on topological interactions in polymers. Macromol. Symp. 117, 233.

Massiera, G., Ramos, L., and Ligoure, C. 2002. Role of the Size Distribution in the Elasticity of Entangled Living Polymer Solutions. Europhys. Lett. 57 127.

Massiera, G., Ramos, L., Pitard, E., et al. 2003. The Steric Polymer Layer of Hairy Wormlike Micelles. J. Phys.: Condens. Matter 15 S225.

Mathis, S. P., Pitoni, E., Ripa, G., Ferrara, G., Conte, A. and Ruzic, M. 2002. VES Fluid Allows Minimized Pad Volumes and Viscosity to Optimize Frac-Pack Geometry: Completion Type Evolution in Barbara Field, Central Adriatic Sea. Paper SPE 78317 presented at the SPE European Petroleum Conference, Aberdeen, Scotland.

McElfresh, P., Williams, C. F., Wood, W.R. 2003. A Single Additive Non-ionic System For Frac Packing Offers Operators a Small Equipment Footprint and High Compatibility with Brines and Crude Oils. Paper SPE 82245 presented at the SPE European Formation Damage Conference, The Hague, The Netherlands.

Nasr-El-Din, H.A., Samuel, E., and Samuel, M. 2003. Application of a New Class of Surfactants in Stimulation Treatments. Paper was presented at the SPE International Improved Oil Recovery Conference in Asia Pacific, Kuala Lumpur, Malaysia.

Nelson, E.B., Lungwitz, B., Dismuke, K., et al. 2005. Viscosity reduction of viscoelastic based fluids. US Patent No. 6,881,709.

Nettesheim, F., Liberatore, M.W., Hodgdon, T.K. et al. 2008. Influence of

Nanoparticle Addition on the Properties of Wormlike Micellar Solutions. Langmuir 24 (15): 7718-7726. DOI: 10.1021/la800271m.

Pashley, R.M., Karaman, M.E. 2004. Applied Colloid and Surface Chemistry. West Sussex, UK: Wiley & Sons. Ltd.

Pourafshary, P., Azimipour, S.S., Motamedi, P., et al. 2009. Priority Assessment of Investment in Development of Nanotechnology in Upstream Petroleum Industry. SPE 126101, SPE Saudi Arabia Section Technical Symposium, Al Khobar, Saudi Arabia.

Propylene Glycol. MSDS No: P355-1. Fisher Scientific: Fair Lawn, NJ. November 19, 2009.

Ramsden, J.J. 2011. Chapter 1 - What Is Nanotechnology? In Nanotechnology, Oxford: William Andrew Publishing.

Rehage, H., Hoffmann, H. 1988. Rheological Properties of Viscoelastic Surfactant Systems. J. Phys. Chem. 92, 4712.

Rehage, H., Hoffmann, H. 1991.Viscoelastic Surfactant Solutions : Model Systems fro Rheological Research, Mol. Phys. 74, 933 – 973.

Rojas, M.R., Müller, A.J., and Sáez, A.E. 2008. Shear Rheology and Porous Media Flow of Wormlike Micelle Solutions Formed by Mixtures of Surfactants of Opposite Charge. Journal of Colloid and Interface Science 326 (1): 221-226. DOI: 10.1016/j.jcis.2008.07.022.

Samuel, M., Card, R.J., Nelson, E.B., et al. 1997. Polymer-free Fluid for Fracturing. Paper SPE 38622 presented at the SPE Annual Conference and Exhibition, San Antonio, TX. DOI: 10.2118/38622-MS

Samuel, M., Card, R.J., Nelson, E.B., et al. 1999. Polymer-Free Fluid for Fracturing Applications, SPE Drilling and Completion, Vo.14. No.4. 240-246, ISSN 10646671.

Schramm, L.L. 2005. Emulsions, Foams, and Suspensions: Fundamentals and Applications. Wiley-Vch Verlag GmbH & Co. KGaA, Weinheim, Germany.

Spenley, N.A., Cates, M.E., and McLeish, T.C.B. 1993. Non-linear Rheology of Wormlike micelles. Physical Review Letters 71, 939.

Spenley, N.A., Yuan, X.F., and Cates, M.R. 1996. Nonmonotonic constitutive laws and the formation of shear banded flows. J. Phys. II 6, 551.

Tadros, T.F. 2007. Colloid Stability, Volume 1: The Role of Surface Forces. Wiley-Vch Verlag GmbH & Co. KGaA, Weinheim, Germany.

Tadros, T.F. 2009. Colloids and Interface Science Series, Volume 5: Colloids and Agrochemicals. Wiley-Vch Verlag GmbH & Co. KGaA, Weinheim, Germany.

Tadros, T.F. 2010. Rheology of Dispersions. Wiley-Vch Verlag GmbH & Co. KGaA, Weinheim, Germany.

Tanford, C. 1980. The Hydrophobic Effect: Formation of Micelles and Biological Membranes. Somerset, NJ: John Wiley & Sons.

Turner, M.S., Cates, M.E. 1990. J. Phys. France, 51, 307.

Van Zanten, R. 2011. Stabilizing Viscoelastic Surfactants in High-Density Brines. Paper SPE 141447 presented at the SPE International Symposium on Oilfield Chemistry, The Woodlands, TX. DOI: 10.2118/141447-MS.

Vashisth, C., Whitby, C.P., Fornasiero, D., et al. 2010. Interfacial Displacement of Nanoparticles by Surfactant Molecules in Emulsions. Journal of Colloid and Interface Science 349. 537-543.

Wagner, N.J., Brady, J.F. 2009. Shear Thickening in Colloidal Dispersions. American Institute of Physics, S-0031-9228-0910-010-8.

Weaver, J., Schmelzl, E., Jamieson, M. et al. 2002. New Fluid Technology Allows Fracturing without Internal Breakers. Paper presented at the SPE Gas Technology Symposium, Calgary, Alberta, Canada. SPE-00075690. DOI: 10.2118/75690-ms.

Yu, J., Berlin, J.M., Lu, W. et al. 2010. Transport Study of Nanoparticles for Oilfield Application. Paper presented at the SPE International Conference on Oilfield Scale, Aberdeen, UK. SPE-131158-MS. DOI: 10.2118/131158-ms.

Zaman, A.A., Singh, P., and Moudgil, B.M. 2002. Impact of Self-Assembled Surfactant Structures on Rheology of Concentrated Nanoparticle Dispersions. Journal of Colloid and Interface Science 251 (2): 381-387.

Zana, R. 2005. Dynamics of Surfactant Self-Assemblies: Micelles, Microemulsions, Vesicles, and Lyotropic Phases. Boca Raton, Florida, USA: Taylor & Francis Group.

Zhang, Y., Cremer, P.S. 2006. Interactions between macromolecules and ions: the Hofmeister series. Current Opinion in Chemical Biology, 10:658–663.

Zinc Oxide Powder. MSDS. Inframat Advanced Materials, LLC: Manchester, CT. July 22, 2008.